THE UNIVERSITY OF HUDDERSFIELD

School of Computing and Engineering

Department of Mechanical Engineering

Flow Non-Uniformity(Φ) In Ducts with Single Inlet and Multiple Outlets

A thesis submitted in partial fulfilment of the requirements for the award of Master of Science Degree in Master by Research

AEMAD GADOUR (U1553108)

MARCH 2022

COPYRIGHT

I. The author of this thesis (including any appendices and /or schedules to this thesis) owns any copyright in it (the Copyright) and he has given The University of Huddersfield the right to use such copyright for any administrative, promotional, educational and /or teaching purposes.

II. Copies of this thesis, either in full or in extracts, may be made only in accordance with the regulation of university library. Details of thesis regulations may be obtained from the Librarian. This Page must form part of any such copies made.

III. The ownership of any patent, designs, trademarks, and all other intellectual property rights except for the Copyright (the Intellectual Property Right) and any reproductions of copyright works, for example graphs and tables, ich may be described in this thesis, may not be owned by the author, and may be owned by third parties. Such Intellectual Property Right and Reproductions cannot and must not be made available for use without the prior written permission of the owner(s)of the relevant Intellectual Property Right and/or Reproduction

ABSTRACT

There have been several studies of flow distribution in manifolds to optimise flow uniformity; however, these attempts have shown that limited advanced had been achieved and more research is required to deeply understand the flow non-uniformity. This work aims to attain equal flow rate at all outlets for a duct of one inlet and ten outlets. There has been a numerical investigation carried out using CFD analysis to provide an analysis of 3D incompressible and turbulent flow to contribute to resolving the flow distribution case. There have been ten simulations performed to understand the non-uniformity and understand the flow behaviour inside the duct.

DECLARATION

This work is submitted to the university of Huddersfield for the fulfilment of Master by Research degree. I declare that the work in this thesis was conducted according to the university regulation. This work is original and has not been submitted for a diploma, degree, or any other qualification at any other educational institution.

DEDICATION

I dedicate this thesis to my parents who have been struggling to survive the conflict back home for the last 7 years and for the unconditional support they give every day to keep going forward and achieve my dreams.

ACKNOWLEDGEMENT

Firstly, all praise and glory to the almighty God who has given me ability, strength and knowledge to continue this research while seeing my family struggling back home from war and poverty. I would also like to send my propound gratitude to **Prof Fengshou Gu** who have been excellent at supporting and encouraging me after the leave of my main supervisor. I would also like to send great thanks to **THE UNIVERSITY OF HUDDERSFIELD** for providing me with such a great opportunity by sponsoring me. To my brothers, sisters and everyone who gave me any advice or supported me I say thank you very much without you I could never do this.

Table of Contents

COPYRIGHT 1

ABSTRACT 2

DECLARATION 3

DEDICATION 4

ACKNOWLEDGEMENT 5

Table of Contents 6

Table of Figures 9

Table of Tables 11

CHAPTER ONE 13

1- Introduction 13

1.1 The Flow Distribution Affecting Parameters 24

1.2 Governing Equations 31

1.3 k-epsilon Transport Equations 32

1.4 Flow Non-Uniformity 33

1.5 Aims and Objectives 34

CHAPTER TWO 35

2-Numerical modelling 35

2.1 Geometry shape and measures justification 37

2.1.1 CAD model 38

2.2 Mesh Sensitivity Analysis 40

2.2.1 Possible Numerical Errors 40

2.2.2 Physical approximation 40

2.2.3 Turbulence error 41

2.2.4 Computer Round-Off Error 41

2.2.5 Iterative Convergence Error 41

2.2.6 Discretization Errors 42

2.2.7 Truncation Error 43

2.2.8 Usage Errors 44

2.3 Mesh Study 1 45

2.4 Mesh Study 2 46

2.4.1 Mesh Quality 48

2.4.2 Mesh Selection Justification 49

2.5 CFD Approach 50

2.6 ANSYS Simulation 51

CHAPTER THREE 54

3- Results 54

3.1 Simulation (1m/s Inlet Flow Velocity) 54

3.2 Simulation (2m/s Inlet Flow Velocity) 55

3.3 Simulation (2m/s Inlet Flow Velocity) 56

3.4 Simulation (4m/s Inlet Flow Velocity) 57

3.5 Simulation (5m/s Inlet Flow Velocity) 58

3.6 Reynolds Number Calculations 59

CHAPTER FOUR.....60

4- Research Findings.....60

4.1 Flow Distribution Design 2.....60

4.2 Flow Distribution Design 2.....61

4.3 Non-Uniformity Coefficient Design 1(Φ).....63

4.4 Non-Uniformity Coefficient Design 2(Φ).....64

4.5 Effect of outlet on Flow Distribution.....65

4.6 Area ratio effect.....68

4.7 Inlet Flow rate effect on non-uniformity.....70

4.8 Results comparison.....72

CHAPTER FIVE.....74

5-Conclusion.....74

5.1 Future work.....75

REFERENCES.....76

Table of Figures

Figure 1: Types of manifolds (Wikipedia 2019)....14

Figure 2: Velocity Distribution Contour (Ansys, 2019)....21

Figure 3: Flow Non-uniformity (Alawee, 2014)....33

Figure 4: Design 1 side view (SolidWorks,2020)....38

Figure 5: Design 2 side view (SolidWorks,2020)....38

Figure 6: 3D view of the duct (SolidWorks,2020)....39

Figure 7: Named Selections Feature (Ansys workbench,2020)....39

Figure 8: Mesh study Design 1 (Mass Flow Rate vs Number of elements)....47

Figure 9: Mesh Study Design 2 (Mass Flow Rate vs Number of elements)....47

Figure 10: Mesh Quality Metrics Skewness and Orthogonal. (ANSYS,2015)....48

Figure 11: Mesh 5 Orthogonal quality and Skewness Design 1 (ANSYS, 2021)....49

Figure 12: Naming Faces using Named selection Feature (Ansys, 2021)....51

Figure 13: Creating Mesh using the Suitable Mesh Size (Ansys. 2021)....52

Figure 14: Applying Boundary conditions (Ansys, 2021)....53

Figure 15: Iterations Number Set-Up (Ansys, 2021)....53

Figure 16: Mass Flow Distribution Line Design 1 vs Design 2....54

Figure 17: Mass Flow Distribution Line Design 1 vs Design 2....55

Figure 18: Mass Flow Distribution Line Design 1 vs Design 2....56

Figure 19: Mass Flow Distribution Line Design 1 vs Design 2....57

Figure 20: Mass Flow Distribution Line Design 1 vs Design 2....58

Figure 21: Reynold Number Flows (Hyper, 2021)....59

Figure 22: Design 1 Flow Distribution Line for 5 Inlet Flow Velocities....60

Figure 23: Design 2 Flow Distribution Line for 5 Inlet Flow Velocities....61

Figure 24: Flow Distribution Pie Design 1....62

Figure 25: Flow Distribution Pie Design 2 62

Figure 26: Low Pressure Distribution Design 1 65

Figure 27: Increase in Pressure Distribution Contour Design 2 66

Figure 28: Design 1Velocity Distribution 66

Figure 29: Outlet Reduction Effect on Flow Velocity 67

Figure 30: Area Ratio Effect on Non-Uniformity 68

Figure 31: Inlet Flow Speed Impact on Non-uniformity Design 1 71

Figure 32: Inlet Flow Speed Impact on Non-uniformity Design 2 71

Figure 33: Design 1 Flow Distribution vs Design 2 Flow Distribution 75

Tables

Table 1: Mesh Convergence Study 1(Flow Distribution at each outlet).....45

Table 2: Mesh Convergence Study 2 (Flow Distribution at each outlet).....46

Table 3: Mesh Quality Metrics for Design 1 (ANSYS, 2021).....48

Table 4: Mesh Quality Metrics for Design 2 (ANSYS, 2021).....48

Table 5: Simulation Parameters (Ansys, 2021) 50

Table 6: Flow Distribution Simulation Results Design 1 vs Design 2 54

Table 7: Flow Distribution Simulation Results Design 1 vs Design 2 55

Table 8: Flow Distribution Simulation Results Design 1 vs Design 2 56

Table 9: Flow Distribution Simulation Results Design 1 vs Design 2 57

Table 10: Flow Distribution Simulation Results Design 1 vs Design 2 58

Table 11: Reynold Numbers 59

Table 12: Mass Flow Rate Distribution Results Design 1 60

Table 13: Mass Flow Rate Distribution Results Design 2 61

Table 14: Non-Uniformity Coefficient Design 1 63

Table 15: Non-Uniformity Coefficient Design 2 64

Table 16: Inlet Flow Rate Effect on Non-Uniformity Design 1 70

Table 17: Inlet Flow Rate Effect on Non-Uniformity Design 2 70

Nomenclatures

u	Axial velocity (x-direction)	*m/s*
v	Transverse velocity (y-direction)	*m/s*
w	Transverse velocity (z-direction)	*m/s*
$\dot{m}$	Mass flow rate	*Kg/s*
k	Turbulence kinetic energy	m^2/s^2
p	Pressure (static)	N/m^2
Dh	Duct Hydraulic diameter (Inlet)	*m*
dh	Outlet Hydraulic diameter	*m*
Qi	Volume flow rate at the i outlet	m/s^3
Q	Total Volume flow rate	m/s^3
N	Number of outlets	
βi	Flow ratio for *i*th outlet	
$\bar{\beta}$	Average flow ratio for all outlets	
L	Length of Duct	*m*
H	Length of outlets	*m*
S	Distance between outlets	*m*
Re	Reynolds number	
ρ	Density of a fluid	kg/m^3
μ_t	Turbulent Viscosity	*kg/ (m.s)*
μ_{eff}	Effective Viscosity	*kg/ (m.s)*
A.R	Area Ratio	
ε	Turbulent energy	m^2/s^3
$C1\varepsilon$, $C2\varepsilon$, $C3\varepsilon$	K-epsilon transport equation constants	
CFD	Computational Fluid Dynamic	

CHAPTER ONE

Introduction

Flow in manifolds is one of the most important factors in many industrial applications especially when it comes to distributing a significant amount of fluid stream into multiple parallel streams that will then be collected into the discharge stream at the end. Many applications where flow distribution contributes directly towards their performance starting from traditional applications such as engines of automobiles and irrigation, until nowadays high-performance devices such as heat exchangers, fuel cells, electronic devices, cooling and radial flow reactors thus optimising such applications is required (Jameson, 2008). It is very important to carry out additional research studies to understand the physics and the nature of flow non-uniformity inside such complex systems. Both fluid-dynamic and thermal performance are affected mainly by flow distribution which is very likely to result in system failure. Several studies have been conducted over decades to identify the causes of non-uniformity and most concluded that non-uniformity is as a result of a great number of variables that act at simultaneously. Inlet flowrate, size of inlet, size of parallel outlets, inlet port size and location to the duct, shape of the parallel outlets and the duct all these parameters play a role in flow non-uniformity (Jameson, 2008). There are numerous types of manifolds to distribute flow such as combining, parallel, dividing and reverse. Parallel manifolds are known as the most used type in the industry of heat exchangers as it combines, divides and combines flow again. Both dividing and combining manifolds have the same flow directions which is normally referred to as Z-manifolds. In the U-manifolds the flow direction is not the same (opposite) which is normally referred to as a U-manifold.

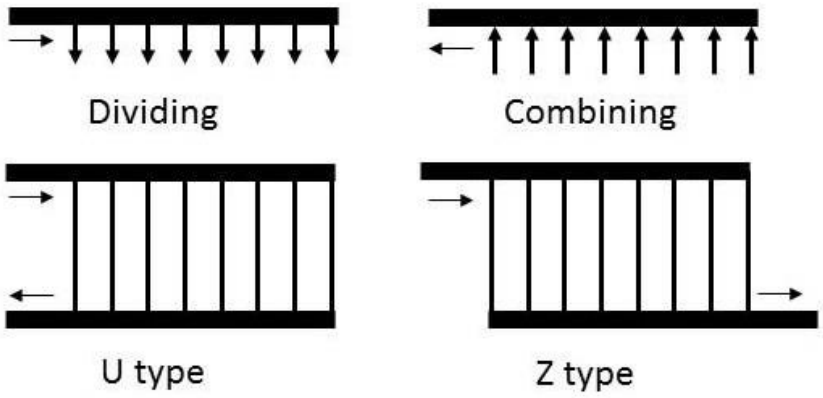

Figure 1: Types of manifolds (Wikipedia 2019)

Furthermore, it is considered that uniform flow distribution requirements are difficult to achieve in different technical applications due to their varying performance in fluid devices including plate heat exchangers, various piping systems, electronic equipment, fuels cells, etc. Consequently, it has been found in the research that for the majority of applications multiple designs are considered the best way of achieving a uniform flow distribution at all outputs. Numerous experimental, analytical, and numerical studies involving various forms of flow distribution have been carried out. Durbin (2010) devised the first general theoretical framework to study the effectiveness of single-phase flow distributions for the intake and exhaust manifold. The main concern is that the side tubes form a sharp edge configuration perpendicular to the axis of the distributor (Jameson, 2008). The mathematical model is formulated as a balance of pulses throughout the variety Bajura and Jones (1976) extended the flow and pressure in the collector to the partial structure of the earlier framework and the prediction, combined with the torsional and parallel manifold, Datta and Majumdar (1980) devised a model with one-dimensional elliptical resolution method while sharing and combining the flow feeder flow predictions. They used mathematical models to numerically study the distribution of parallel and counter current varieties. In both studies, the authors found two dimensionless parameters (surface parameters and friction parameters) that affect the distribution of the flow . Analytical and

experimental studies were carried out of the flow distribution of parallel and counter current and air varieties. They discovered that the counter current distributor offers a more uniform flow distribution than the parallel flow distributor in the same geometric and operational conditions. Mueller and Chiou (1988) presented the factors that influence the misconfiguration of heat exchangers in a review article. Hoerner (2012) declared that the distribution of flow from the collector has become a concern to forecast the transmission of heat progress of the compact heat exchanger. In general, traffic flows through the channel, which is not uniform under extreme conditions, while others barely work, resulting in poor heat exchange performance. Choi et al (1993) in a group study have numerically considered the surface ratio impact on the flow distribution in a distributor of liquid cooling modules of electronic components. The study has shown that the flow rate of the last outlet is 2.75 times greater than that of the first outlet . The study concluded that the surface ratio of the most important parameters affects the distribution of the refrigerant and must be carefully considered during the construction of the liquid cooling module. Kim et al (1995) Investigated the shape of the digital survey head and the flow rate of the parallel flow distributor of the liquid cooling module for the electronic component are assigned to the Reynolds number of the geometry of the three different geometries (i.e., rectangular heads, triangular and trapezoidal) for the direction of flow Z. The results show that the shape of the triangle is distributed optimally regardless of the entry speed. The influence of the angle of the inlet head and the mass flow in the flow distribution has been studied experimentally together with the optimized design of the plate and fin heat exchanger. The results show that the best flow distribution can be obtained when the angle of incidence is 45 ° V. Hoerner (2012) examined the consequence of the inlet tube diameter, the first equivalent surface collection diameter, and the second equivalent surface collection diameter of the irregular flow dissemination in heat exchangers. To decrease the uneven distribution of flows in the manifold of a heat plate, the author proposes a modified header configuration . A second collector (B or C) was installed after the first collector to verify the distribution of the flow. McNown (2008) developed a mathematical model to optimize the rectangular variety. The results of the simulation show that the longer derivation channels allow a

uniform distribution of the liquid in each channel. It also shows that the expansion of the exhaust manifold region makes the distribution of the flow uniform. The experimental results show that the uneven distribution of the flow is very severe in the conventional dispensing head and that the improved dispensing head can effectively improve the uniformity of the perforated baffle.

Tong et al (2009) carried out a number of strategies that can be used to achieve the same massive output through each manifold output. The results show that the objectives of uniformity of runoff is the most effective.

a) Widening the cross section of the dispenser.

b) Modification of the section of the download step.

c) Linear iconicity of the distributor section.

d) Reduce the cross section of the distributor in a non-linear manner by following an elliptical profile of a quarter of the distributor wall.

It is considered that a three-dimensional model of computational fluid dynamics (CFD) is used to calculate the velocity distribution between a plurality of parallel micro channels having a triangular variety (Durbin 2010). The results of the simulation show that the greater the length, depth or width of the micro channel, the more uniform distribution of the speed will be. Tong and Sparrow (2009) have proposed a method to study the effect of output geometry on uniformity of mass flow away from the variety. Mass output results per port are normalised to the average mass flow of the collector, which indicates that the performance of a single continuous tank is optimal. They useda logic-based system approach to design the distribution system to achieve a uniform flow between the channels connecting the two collectors.This method involves adjusting the flow resistance of each channel to achieve the same pressure loss for all channels. Hanfei Tuo and Pega Hrnjak (2013) studied an experimental and numerical way to show the insufficiency of the flow distribution caused by the pressure drop in the collector and its effect on the performance of the micro channels of horizontal

and vertical directional tubes. Experimental results indicate that the flash gas bypass process virtually eliminates distribution inequalities related to quality. In recent years, numerous articles published responses using global kinetics without considering the diffusion of coatings (Anderson 2009). The actual inclusion of reactive chemicals is a major challenge in the modelling of converters. This includes mass and energy balance equations using cold flow simulations and the transient flow distribution in the catalyst. The uniformity of the flow in the CATCON substrate depends on not only the exhaust manifold, the design of the inlet and outlet cones, but also on the size and configuration of the substrate (Anderson 2009). There is no consistently optimized conical design for different catalysts, but the optimization of the inlet cone ensures a smoother flow. Today, CFD can more accurately predict the results of complex processes and has become the most important process optimization tool.

It is important to understand the effect of the operational constraints on the distributions of the flows during each analysis through experimental models and CFD. Nevertheless, only a few research have been conducted on specific categories of experimental heat exchangers. The unequal distribution mechanism of the flow between the tubes of the heat exchangers must be carefully examined to determine the main parameters at the origin of this unequal flow distribution (Guo Jiang & Song, 2005). The misalignment of the flow in the collector can be affected by the direction of the collector, the speed of entry and the geometry. The main purpose of the design of heat exchangers is to achieve a uniform distribution of the flow in the tubes of the heat exchanger to attain heat exchangers with uniform cooling. Furthermore, it is considered the experimental study of the effects of the first and second detection diameters of the uneven distribution of the plate heat exchanger (PFHE) in the diameter and inflow. The correlation between the parameters of the incorrect dimensional flow distribution and the Reynolds number is obtained in several configurations.

Furthermore, it has been observed that many numerical models are required in order to understand the unequal distribution of flows. Durbin (2012) describes several models that deal with uneven distribution of plate heat exchangers and cross current heat exchangers. His work solved the equations using the inverse numerical transformation and transformation algorithms. They show that the effect of the lateral thermal resistance of the fins in the heat exchanger with aluminium fins on the temperature and the misalignment of the flow is negligible and is attributed to a high efficiency of the fins. A study was conducted by using a finite element process of Plattenrippen and cross-flow compact heat exchangers, the effect was to consider the unequal distribution of the heat exchangers wall and the flow of input fluid at two temperatures, in addition to the two-dimensional thermal conduction on the cold side and longitudinal direction of the heat exchanger. The mathematical equations for different types of input and erroneous temperature distribution are solved using finite element codes. On this basis, the efficiency of the heat exchanger and its deterioration due to poor application of flow rate was measured. (Durbin, 2012). It has been observed that there is a significant

impact on the loss of performances of the heat exchangers due to uneven distributions of flow and temperature. Anderson (2009) has studied the influence of the unequal distribution of the flows on the thermal efficiency of the cross-flow heat exchanger and the weakening or promotion because of the unequal flow distribution. They note that the optimal mismatch mode improves the thermal efficiency of the crossflow heat exchangers when the number of transmission units (NTU) and the heat capacity ratio are considered to be large. The research by Rao (2007) showed that the optimal designing of the distributor structure could significantly improve the distribution of the flow in the plate heat exchanger. Rao and his colleagues have described a better way to analyse heat transfer data from plate heat exchangers. Hendrickson, et al (2013) provided details based on the correlation of the numerical study of the irregularity parameter of the flow distribution of the air flow heat exchanger and noted that the Reynolds number of the inflow and the geometry of the nozzle significantly influence the irregularity of the flow distribution. In addition, the results indicate that a reduction in the diameter of the nozzle leads to an increase in the incorrect application of the flow rate . It was found that increasing the number of nozzles did not significantly affect the distribution. The results show that the inclusion of the second heading tends to reduce the unequal distribution of the flow. The CFD examination of the two phased refrigerant flow in the horizontal pipeline was performed under adiabatic conditions using a homogeneous model. Recently, Hendrickson, et al (2013) investigated the uneven distribution of flows in air-cooled heat exchangers. The study assessed the effect of the numbers of nozzles, their position, their geometry and their diameter in a bad configuration in the heat exchangers. In various applications of energy conversion in plate heat exchangers, chillers are used as power plants, petrochemical plants, and transport vehicles. They exchange thermal energy amid two fluids with diverse flow temperatures. Most of the energy transfer occurs in these types of heat exchangers used in various applications. The large amount of energy consumed by the heat exchangers used in these applications saves a lot of energy on the efficiency of the fin heat exchangers. Moreover, it is considered that an important benefit of plate and fin heat exchanger over conventional heat exchangers is that the fluid is exposed to a larger surface as it

extends over the plate. In the construction of a plate and fin heat exchanger, it is commonly accepted that the distribution of the fluid flow is evenly distributed in all the parallel rib-shaped passages through the core of the heat exchanger. However, in practice, it is not possible to uniformly distribute the liquid flow due to a misalignment of the flow (Anderson 2009). The misalignment of the flow is an uneven distribution of the mass flow in the core of the heat exchanger. The uneven distribution of the flow depends on several factors such as the geometry of the heat exchanger (that is, the mechanical design, the geometry, and the dimensions of the channel and manifold, manufacturing tolerances or errors), and the operating conditions (variations in flow throughout the collection). Jian Wen and Yanzhong Li (2007) analysed the unequal distribution of the liquid flows in the heads of the standard collectors and the findings suggest that the collector has three different diameters installed with a small orifice baffle to control the uneven distribution of the heat exchanger. The resulting numerical outcomes effectively increase the performances of the heat exchanger Hendrickson, et al (2013) proposed two improved headings with a two-stage distribution structure to reduce the inhomogeneity of the flow. They have shown that the distribution of fluid flow in the plate heat exchanger is more uniform when the ratio of diameters are equivalent to the output and the input of the two collectorse. They have studied a compact fin plate and a finned heat exchanger considering the combined effect of two-dimensional thermal conduction through the wall of the heat exchanger in the longitudinal direction and with the method of input fluids and finite elements. The temperature distribution is made by an irregular flow. Jiao et al (2003) investigated experimentally the configuration of the collector of distribution of errors in plate and fin heat exchangers. His research shows that by optimizing the multiple configurations, the performance of the flow distribution in the plate and the heat exchanger of the fins is effectively improved. Researchers analysed the distribution of the two-stage flow in a collector with an equivalent inlet diameter in a plate and fin heat exchanger (Anderson 2009). It was verified that the distribution of fluid flow in the plate fin heat exchanger was more uniform when the ratio of the equivalent output and the input diameters of the two sensors was the same. The CFD analysis was performed on three different types of finned heat exchangers to study

the effect of misalignment on the performance of the heat exchanger. Improved collectors have been proposed to improve the incorrect application of the flow of the three heat exchangers. The number of nozzles determines the diameter of the nozzle, as well as the geometry and position of the nozzle and the inflow, the second manifold is included with the flow distribution of the heat exchanger tubes of the heat exchanger. The results show that the inclusion of the second collector represents a significant reduction in the unequal distribution of the flow. In the present work, an improved intention of deflectors that have different arrangements has been proposed i.e. the number of checks of the behaviour of the flow in the modified header, the CFD software, FLUENT, analyses of four types of plate collectors and finned heat exchangerso study the uneven distribution of the flows. The inlet tube has a diameter of 200 mm, the collector has a radius of 154 mm, and the current collector has a length of 905 mm (Durbin 2010). Housing 2 is a two-channel head with an inline stamped baffle inserted between the heads. The holes in the deflectors have three different diameters, as shown in Figure 2 (a), in which an in-line whole arrangement is used. The diameters of the holes used were 10 mm, 20 mm and 30 mm, respectively.

There are several numerical and analytical studies that have been carried out recently regarding flow distribution in systems with single inlet and multiple outlets. The beginning was with the developed theoretical model by which the performance of single-phase flow distribution of two types of manifolds intake and exhaust can be investigated. The study focused on the manifold configuration in

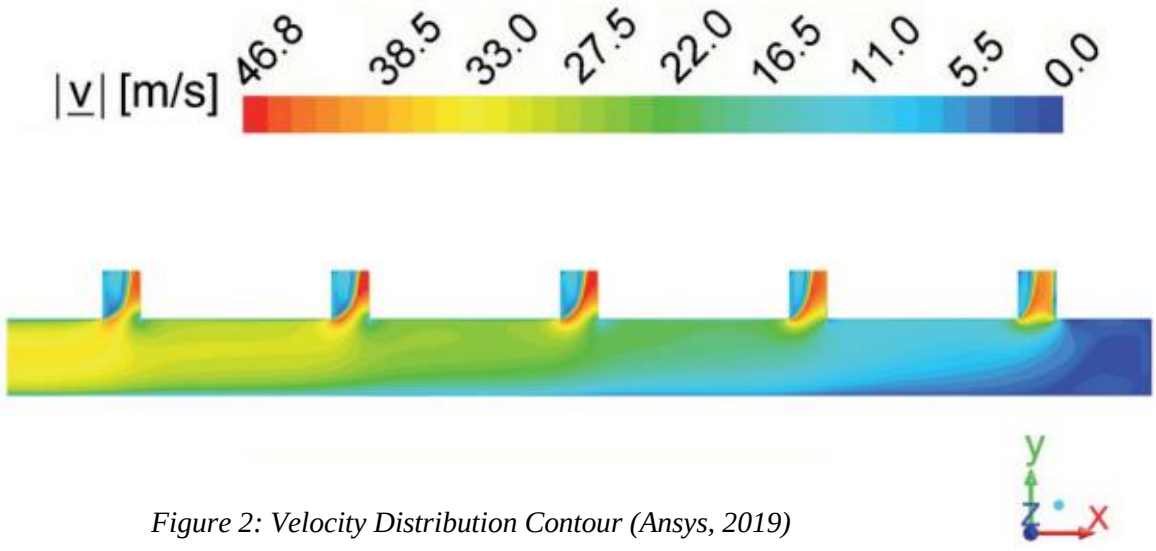

Figure 2: Velocity Distribution Contour (Ansys, 2019)

which the outlets at 90 degrees bend with the axis of the manifold. As a result of the momentum balance along the pipe a mathematical model was created. The study was then extended for the previous model to predict the header pressure and flow rate for the dividing, combining, reserve and parallel manifold systems. It was found that flow uniformity in the outlets is attained once the header work as an infinite reservoir. Area ratio, outlets flow resistance, length of header, diameter of header and the friction factor were identified as the most effective parameters towards the flow distribution along the manifold. A developed mathematical manifold with 1-D elliptic solution procedure for studying flows in dividing and combining flow manifolds (Durbin 2010). A numerical investigation of parallel and reserve manifold has been also carried out using the same mathematical model. stated that for both investigations the flow distribution was mainly affected by area ratio and friction. An analytical and experimental study of the air flow in reserve and parallel manifold with the same geometrical and operating conditions was conducted, the study showed that the parallel manifold provides less uniform flow than the reserve manifold . An article has been approached to review the influencing parameters regarding flow distribution in heat exchangers. Jameson (2008) stated that "The flow distribution from manifold has become of interest in predicting the heat transfer performance of compact heat exchangers". Generally, the flow rate through the outlets is not uniform and, in most cases, some outlets has no flow at all in them which lead to poor performance . The friction impact on flow uniformity in dividing and combining flow systems has been evaluated and led to an analytical solution. An assumption of constant manifold header area and constant friction factor was made to solve the case. Friction and momentum loss were the two expressed parameters for the outlets flow distribution. For the combining flow manifold the flow imbalance was increased by the friction. However, for the dividing flow manifold, the flow imbalance may decrease or increase depending on the outlets area ratio to the manifold header area. A numerical study has been carried out to investigate the area ratio effect on the flow distribution for a liquid cooling manifold. The investigation stated that the flow distributed in the last outlet was 2.6 times the flow rate than that in the first outlet. Anderson (2009) concluded that ''the area ratio is one of the most important

parameters affecting the coolant distribution and should be carefully examined in the design of a liquid cooling module''. has also numerically investigated Reynolds number and width ratio effect on the flow distribution for the same liquid coolant configuration. The results found out that the two parameters play a significant role on improving the flow distribution where results improved by increasing the width ratio. However, higher Reynolds number led to less flow rate in the first outlets and more flow in the last outlets. The shape of the header and Reynold number effect was numerically studied by the z-type flow direction and with three types of manifold geometries: rectangular, triangular and trapezoidal. The study concluded that the inlet flow velocity has no effect and the best flow distribution was provided by the triangular geometry where the velocity was assumed to be uniform at the header. Slight similar flow distribution was provided by the trapezoidal geometry, the rectangular geometry produced the worst flow distribution by providing the last outlet with the highest flow rate resulting in flow non-uniformity. Anderson (2009) calculated the dividing flow manifold hydraulics using the spread sheet program. A circular manifold with 101.5 mm diameter to distribute a flow of 50.95 into 5 consecutive outlets of 50.7 mm diameter that oriented with 90 degrees angle with manifold header axis. The aim was to calculate flow distributed at each of the outlets, considering the assumption that ' the head loss in the energy line from manifold through lateral is the same at every point'. The researcher found a solution for two types of manifolds, in the first case the manifold diameter was fixed and remained constant, in the second case the manifold dimeter was variable and reduced from 0.125m to 0.056m. The constant diameter resulted in lower flow distribution all over the manifold where the flow rate in the first outlet was 55% less than the flow rate in the last outlet. However, the varying dimeter manifold improved the flow distribution and led to nearly equal flow rate at all the outlets. A computational model was developed by Anderson (2009) to predict the flow distribution for flow spreaders manifold types, many numerical processes and technique are used to solve complex manifold geometries and configuration, such as the flow spreader manifold which can be found in most industrial applications of head box for paper-making systems. ''The major effort in the work is to use and generalized multi- grid elliptic grid generation program

to create grids for the tapered manifold spreader with different cross-sectional configurations, especially for the manifolds with a circular cross section'' (Jiao, 2003). CFD code was used to compute many 2D and 3D turbulent and laminar flows and validate the results with any other recent numerical, experimental and analytical studies. The results that were presented for the laminar flow actually agreed with the literature and the recirculation rate impact on the manifold flow distribution was studied. The results indicated that flow rate at the manifold down-stream dropped significantly using the 10% recirculation rate, with the zero recirculation rate results show pressure increasing and significant flow rate at the outlets closer to the manifold dead-end. Jiao (2003) carried out a numerical study using CFD to compute three-dimensional steady flow and pressure for a T-junction connected geometry with three risers which comprises dividing and combining flow. The standard and RNG k-s models have been selected to ensure that their integral model is benchmarked for flow distribution. An agreement was obtained for both approaches which proved that flow distribution is one of the predictable large-scale features of 3D branching flows. Not to mention the quality effect, the study of flow distribution for a single-phase flow application is nevertheless limited (Jiao, 2003).

1.1 The Flow Distribution Affecting Parameters

There are several factors and parameters that influence the flow distribution. A theoretical modelling approached using the electrical resistance network form in the optimisation of trapezoidal geometry, obtaining flow uniformity among micro channels (Bajura and Jones 1976). Numerical simulations validity was checked against calculated results. Similar relationship to the law of Ohm's was established by the approached model for pressure drop, flow rate and flow resistance. The only considered parameter was wall friction as all pressure losses in the manifold were neglected because of the branching effects. Linear relationship was established between flow rate and pressure drop. Parameters affecting flow uniformity for plate fin heat exchanger such as inlet angle and mass flow rate were experimentally investigated to optimise the geometry design. The obtained results indicated that 45 degrees angle of an inlet has led to the optimum flow distribution. It was also found that the

inlet angle results in minimal effects on pressure drop. It was also noticed that Reynolds number is the only parameter that pressure drop depends on (Bajura and Jones 1976). The flow distribution in plate fin heat exchanger is predicted using the developed computational model by Bajura and Jones (1976). Results show that flow non-uniformity is very significant in the y direction of the conventional header. The simulation was carried out using the current plat-fin heat exchanger. The experimental calculation showed an agreement with the numerical prediction. A simulation of two modified headers for two stage distributing structure were conducted in this paper. The effects of inlet dimeter for the two-stage configuration have been investigated and compared with the results that is experimentally produced. It was found that when the inlet and outlet ratios of the heat exchanger plate are equal the flow is nearly uniform all over the structure (Pigford, Ashraf et al. 1983). Inlet manifold size, header one size and header two size effects on the flow distribution of the plate-fin heat exchanger have been experimentally investigated by Mueller (1988). The header configuration was modified as suggested by the author, a second header (B or C) was installed just after the first header to investigate the distribution of the flow velocity. Between the first and the second header there is a connection part where header B has 5 holes and header C has 7 holes. It was found that the flow was significantly improved using the modified configuration as header C led to the most uniform velocity distribution over all considered cases. (Mueller 1988). The optimisation of a rectangular manifold was carried out by Shen (1992) after a computational model was developed. It was found that longer branched outlets resulted in better flow distribution through all channels. Furthermore, it was noticed that uniformity increases as the outlet manifold area is magnified. However, this magnification in manifold outlet area also results in the dead volume inside the micro device to increase residence time distribution to broaden and longer space time. A comparison was carried out for the flow distribution in micro channel structure with triangular manifold between the results of 2D and 3D CFD simulation (Choi, Shin et al. 1993). It was concluded that 2D simulations were significantly accurate compared to 3D simulation when it comes to the correct velocity distribution of flow required. Choi, Shin et al. (1993) conducted a study on the one-dimensional models for inlet and exhaust headers of U and Z

manifold type using mass and momentum balance equations. The models have been compared to the results obtained by three dimensional models so results validation can be obtained. The validation demonstrated that the mild to serve flow non-uniformity was possible in both structures and manifolds for common fuel-cell distributor dimensions. It was also found that non-uniformity (flow maldistribution) strongly depended on the geometrical aspect whereas changes in outlets, header and rip width between outlets can dramatically overturn the whole general results of flow distribution (Ramamurthy, Qu, Vo, & Zhai, 2006). The equations of Reynolds averaged Navier-Stokes (RANS) was applied to 90-degree rectangular dividing flow junctions. The idea was to adopt the 3D k-turbulence model for numerical simulations to achieve dividing flow characteristics. Energy loss coefficient, pressure profile, velocity profile and the mean flow profile are part of these characteristics. The experimental data was used to validate the obtained results as the laser doppler anemometry was the used technique to carry out the experiment and the measurement of velocities in the test section. It was noticed that the experiment agrees with the flow zone separation prediction as the author demonstrated that the model can be used to obtain exit flow rate ratios, area ratios and energy loss coefficient with much less effort (Kim, Choi et al. 1995). Particle image velocimetry (PIV) was used to investigate the flow characteristic in the plate-fin heat exchanger inlet region. The results of the experiment show that flow non-uniformity is very high in the conventional header, whereas flow uniformity increased with the improved structure configuration. The non-uniformity parameter in the plate-fin heat exchanger reduced from 1.20 to 0.22, as well as the ratio between the maximum velocity to the minimum velocity which demonstrated a significant reduction from 23.3 to 1.9. (Pretorius, 1997). A discrete model was formulated to calculate the flow distribution in manifolds. The flow parameters were experimentally evaluated for the discrete model to be supported. The aim was to conduct an experiment with specific conditions that determine pressure distribution in the header. Under specific conditions the theoretical model was validated against the experimental results. Obtaining accurate results needed both refined probes and ultrasonic measuring devices. The results of the experiment have substantially agreed with the theoretical approach. Furthermore, there

were several advantages of accommodating the local disturbances in the discrete model as some of the local disturbances have shown significant effect. The analysis of the study has resulted in realizing in the improvement of the heat exchanger manifolds design that will contribute towards the safety of the operating under severe operational circumstances (Hudson, Uhler et al. 1979). Several strategies were numerically investigated to check whether it's capable of achieving the optimal manifold design and obtain perfect flow distribution through all outlets. The study indicates that attainting equal flow rate through all exits is possible when several objectives are met, these are: (1) enlarge the cross-sectional area of the manifold, (2) variate the cross-sectional area of the outlet, (3) taper (linear) the cross-sectional area of the manifold (Hua, 1998). A three-dimensional simulation of CFD model was performed to determine the distribution of velocity along tringle manifold with multiple parallel outlets. The influence of outlets width and outlets spacing towards the overall flow distribution of U-shape configuration was investigated (Hua, 1998). The results of the simulation indicated that the velocity tended to be more uniform with larger outlet length or smaller width. Horizontal, longitude and width of both inlet and outlet are the main factors that affect flow uniformity and optimising such factors can contribute towards better overall flow distribution through all outlets (Hua, 1998). A method was presented by Commenge, Falk et al. (2002) to carry out an investigation regarding the geometrical effect of the manifold's outlets on the flow uniformity. There were three type of outlets geometries that were considered: (a) circular array, (b) slots array, (c) a single rectangular slot. In order to provide an overall valid comparison of the effect of each individual geometry the outlets area of all geometries was made identical. The results of the mass flow rate of each outlet to the average mass flow rate of the manifold demonstrated that the single rectangular slot provided the best performance from the other two geometries with variations of less than 5%. The circular array and the slots array provide end to end variations with 10% and 15% respectively. The various types of slot geometries have also provided similar pressure rise (Jiao, Li et al. 2003). The flow distribution has also been investigated for a model of complex network comprising various scale under several flow conditions. The study has found that the two-scale configuration produced the

highest flow uniformity (Zhang and Li 2003). A logic-based systematic method was applied to design a manifold achieving flow rate uniformity among all outlets interconnecting a distribution manifold to a collection manifold. The idea was to tailor the flow resistance of each outlet resulting in equal pressure drop at all outlets thus equal flow rate. The outlets were tailored using gate-valve-like obstruction (Zhang and Li 2003). The determination of the optimum variables has been carried out with the examination of an inverse design problem for a 3D Z-type heat exchanger using the method of Levenberg Marquardt for achieving the uniform flow rates (LM) (Jiao, Li et al. 2003). The examination was conducted with five different optimisation problems to provide the study validity. The justification of the obtained results from the LM method was based on numerical experiments. It was stated that the inlet header length and the estimated pipe dimeters can effectively lead to eliminating the eddy flow in the first outlet as a result of the vortex flow circulation near the header inlet. Consequently, the non-uniformity of the flow in the system can be minimised and the flow rate at all outlets inside the heat exchanger is mostly uniform(Jiao, Li et al. 2003). Both numerical and experimental approaches were carried out to investigate the single-phase flow into multiple parallel flow heat exchangers comprising of inlet and outlet, including square cross section and ten circular tubes. The approach was to investigate header size, flow direction Z, flow direction U, area ratio, inlet flow condition, gravity and outlet dimeter. It was concluded that the flow uniformity in the U flow direction is much higher than the Z flow direction. The entrance volumetric flow rate leads the flow ratio at the first outlets to be 50% less than the flow ratio at the last outlet of the Z type flow direction (Tonomura, Tanaka et al. 2004). The fluid flow distribution and heat transfer for microstructure reactors were numerically and experimentally presented by Griffini and Gavriilidis (2007). The investigation focused on how flow non-uniformity affects micro reactors thermal and conversion behaviour. With 5 modified inlet headers (trapezoidal, one multistep, 2 baffle plates and 1 baffle header) and a rectangular, the flow distribution results were experimentally presented for a compact heat exchanger. The inlet header is where a jet stream was induced that associated with vortexes influencing the front tubes flow distribution. It was found that the flow distribution in the header is

depends on the total flow rate and the header form (Maharudrayya, Jayanti et al. 2005). The author concluded that the best performance was presented by the baffle header since the vortexes can be eliminated by this type of header. Ramamurthy, Qu et al. (2006) has also carried out a case study to examine the theoretical model development and the solution methodology regarding flow distribution in manifolds, highlighting all noteworthy advances in the past sixty years. There are three approaches that were reported: CFD approach, analytical model approach and discrete model approach. The author has also noted three parameters that control the manifold flow and pressure distribution (E, M, ζ). Two manifolds structures were used to conduct three-dimensional CFD simulation to compute the velocity distribution among outlets. The results of an obtuse angled manifold were compared to a right-angled manifold, the simulation results did show that for all velocities at the inlet the right-angled manifold lead to more uniform velocity distribution (Wen, Li et al. 2006). Another flow distribution improvement in the manifold performance was noted by Lu, et al. (2008) as the steam reformers have also presented more uniform distribution. Since then, the importance of manifold design has been an essential factor regarding the efficiency of the micro reactor systems. A numerical and experimental approach was carried out to investigate the pressure drop in the headers which causes the flow non-uniformity influencing the micro channel evaporator performance with vertical tubes and horizontal headers. The results of the investigation indicate that the induced flow non-uniformity can be mostly eliminated with the gas bypass (Tong, Sparrow et al. 2009). An experimental approach was conducted to investigate the inlet effect towards two-phase upward branching refrigerant in a heat exchanger. The investigation focused on three types of entrance configurations: normal, parallel, vertical. Results demonstrate that the vertical configuration have produced the best flow distribution among all configurations, parallel configuration was the best for distributing liquid, and to distribute gas the normal configuration was convenient (Pan, 2009). A T-junction of solar collector manifold was numerically analysed using CFD to determine the pressure losses for both combining and dividing flow. The experimental results of U-configuration agreed with

the numerical results. The CFD method can be considered as an alternative of costly experiment in the estimation of Junctions pressure losses (Mathew, John et al. 2009).

1.2 Governing Equations

The equation of mass conservation for a flowing fluid is shown below:

$$\frac{\partial \rho}{\partial t} + \Delta . (\rho U) = 0 \quad (2)$$

Equation 1: The General Conservation of Mass Equation (Makky, 2021).

Equation 2 is known as the general equation which belongs to incompressible flow. Cases with steady 3-D and incompressible flow should be simplified and presented as follows:

$$\frac{\partial u}{\partial x} + \frac{\partial v}{\partial y} + \frac{\partial w}{\partial z} = 0 \quad (3)$$

Equation 2: Continuity Equation for 3-Dimenstional Incompressible Flow (Makky, 2021).

$$\rho\left[\frac{\partial u}{\partial t} + \frac{\partial}{\partial x}(u^2) + \frac{\partial}{\partial y}(uv) + \frac{\partial}{\partial z}(uw)\right] = -\frac{\partial p}{\partial x} + \mu\left[\frac{\partial^2 u}{\partial x^2} + \frac{\partial^2 u}{\partial y^2} + \frac{\partial^2 u}{\partial z^2}\right] + S_u$$

$$\rho\left[\frac{\partial v}{\partial t} + \frac{\partial}{\partial x}(uv) + \frac{\partial}{\partial y}(v^2) + \frac{\partial}{\partial z}(vw)\right] = -\frac{\partial p}{\partial y} + \mu\left[\frac{\partial^2 v}{\partial x^2} + \frac{\partial^2 v}{\partial y^2} + \frac{\partial^2 v}{\partial z^2}\right] + S_v$$

$$\rho\left[\frac{\partial w}{\partial t} + \frac{\partial}{\partial x}(wu) + \frac{\partial}{\partial y}(wv) + \frac{\partial}{\partial z}(w^2)\right] = -\frac{\partial p}{\partial z} + \mu\left[\frac{\partial^2 w}{\partial x^2} + \frac{\partial^2 w}{\partial y^2} + \frac{\partial^2 w}{\partial z^2}\right] + S_w$$

Equation 3: The Momentum Conservation Equations in the x,y and z directions (Makky, 2021).

(4)

$$\bar{u}\frac{\partial \bar{u}}{\partial x} + \bar{v}\frac{\partial \bar{u}}{\partial y} + \bar{w}\frac{\partial \bar{u}}{\partial z} = -\frac{1}{\rho}\frac{\partial \bar{p}}{\partial x} + \frac{\mu}{\rho}\left[\frac{\partial^2 \bar{u}}{\partial x^2} + \frac{\partial^2 \bar{u}}{\partial y^2} + \frac{\partial^2 \bar{u}}{\partial z^2}\right] - \left[\frac{\partial \overline{u'^2}}{\partial x} + \frac{\partial \overline{u'v'}}{\partial y} + \frac{\partial \overline{u'w'}}{\partial z}\right]$$

$$\bar{u}\frac{\partial \bar{v}}{\partial x} + \bar{v}\frac{\partial \bar{v}}{\partial y} + \bar{w}\frac{\partial \bar{v}}{\partial z} = -\frac{1}{\rho}\frac{\partial \bar{p}}{\partial y} + \frac{\mu}{\rho}\left[\frac{\partial^2 \bar{v}}{\partial x^2} + \frac{\partial^2 \bar{v}}{\partial y^2} + \frac{\partial^2 \bar{v}}{\partial z^2}\right] - \left[\frac{\partial \overline{u'v'}}{\partial x} + \frac{\partial \overline{v'v'}}{\partial y} + \frac{\partial \overline{v'w'}}{\partial z}\right]$$

$$\bar{u}\frac{\partial \bar{w}}{\partial x} + \bar{v}\frac{\partial \bar{w}}{\partial y} + \bar{w}\frac{\partial \bar{w}}{\partial z} = -\frac{1}{\rho}\frac{\partial \bar{p}}{\partial z} + \frac{\mu}{\rho}\left[\frac{\partial^2 \bar{w}}{\partial x^2} + \frac{\partial^2 \bar{w}}{\partial y^2} + \frac{\partial^2 \bar{w}}{\partial z^2}\right] - \left[\frac{\partial \overline{u'w'}}{\partial x} + \frac{\partial \overline{v'w'}}{\partial y} + \frac{\partial \overline{w'w'}}{\partial z}\right]$$

Equation 4: Reynold Navier Stokes Equations (Makky, 2021)

(5)

1.3 k-epsilon Transport Equations

The u, v, w presents the three-dimensional velocity components where ρ is density and effective viscosity is determined as follows $\mu_{(\text{effectiveness})} = \mu + \mu_{(\text{turbulence})}$. The selected turbulent model affects the turbulent viscosity as it differs from one application to another. Realizable K-epsilon is the selected model to be used for the present case.

$$\frac{\partial}{\partial t}\left[\rho_{\varepsilon}\right] + \frac{\partial}{\partial x_i}\left[\rho_{ku_i}\right] = \frac{\partial}{\partial x_j}\left[\mu + \frac{\mu_t}{\sigma_k}\right]\left[\frac{\partial_k}{\partial x_j}\right] + G_k + G_b - \rho\varepsilon - Y_M + S_K$$

$$\frac{\partial}{\partial t}\left[\rho_{\varepsilon}\right] + \frac{\partial}{\partial x_i}\left[\rho_{\varepsilon u_i}\right] = \frac{\partial}{\partial x_j}\left[\mu + \frac{\mu_t}{\sigma_k}\right]\left[\frac{\partial_\varepsilon}{\partial x_j}\right] + C_{1\varepsilon}\frac{\varepsilon}{k}\left[C_k + C_{3\varepsilon}\, G_b\right] - C_{3\varepsilon}\rho\frac{\varepsilon^2}{k} + S_\varepsilon$$

Equation 5: Standard k-Epsilon Transport equation (Makky, 2021)

(9)

1.4 Flow Non-Uniformity

It is very important to evaluate the flow distribution using flow non-uniformity coefficient where it helps in obtaining the most suitable design configuration. Flow non-uniformity is a common problem in all fluidic devices for equipment designers. Many researchers have been studying this case to provide the industry with better justifications and explanation. The idea was to create a simple multichannel model to deeply understand how uniformity occur.

Figure 3: Flow Non-uniformity (Alawee, 2014)

The efficiency of flow distribution in manifolds can be determined using the provided equation below which presents two dimensionless factors, Φ and βi.

$$\varphi = \sqrt{\frac{\sum_{i=1}^{n} (\beta_i - \bar{\beta})^2}{N}} \qquad where, \quad \beta_i = \frac{Q_i}{Q} \quad ; \quad and, \quad \bar{\beta} = \frac{\sum_{i=0}^{n} \beta_i}{N} \tag{10}$$

Equation 6: Non-Uniformity Equation (Alawee, 2014)

Lager Φ means lower flow distribution in the system thus lower efficiency where any design with low non-uniformity coefficient can be considered the optimum design configuration for the distribution system. The flow ratio of each outlet is represented by βi,, the flow rate at each outlet represented by Qi and the total flow rate of the system is represented by Q (Choi, 1982). The total number of outlets is represented by N and β is the average flow ratio of the outlets.

1.5 Aims and Objectives

This project aims to consider and understand the physics behind non-uniformity in manifolds and obtain progress in increasing uniformity by providing the optimum design configuration.

This project's requirement is:

- Understand the importance of achieving flow uniformity for such engineering applications.
- Provide study research on recent techniques in improving flow distribution.
- Explain and understand the geometry effects on flow non-uniformity.
- Use CFX ANSYS to carry out several simulations and analyse the flow behaviour under certain circumstances.

However, there are certain objectives that must be accomplished before achieving the mentioned aims.

- To find out real-life problem dimensions for the model creation by conducting online research.
- To create 1:1 scale CAD model using SolidWorks Package.
- To provide the most suitable mesh size by carrying out mesh sensitivity analysis.
- To calculate the mass flow rate at each outlet and create graphs to show flow distribution.
- To increase flow rate at the inlet and note the results to use them for comparison and analysation.
- To measure Reynolds number and non-uniformity coefficient to provide the study with more detailed description.

CHAPTER TWO

Numerical modelling

Computational fluid dynamics (CFD) has emerged as a viable design tool in the industry over the past decades. CFD is a powerful technique for estimating fluids motions within numerous complex systems however, the accuracy of CFD simulations strongly depends on the appropriate setting of boundary conditions and numerical simulation parameters (Giraldo, 2020). Using a numerical model CFD can provide solutions and analysis of any heat-transfer and flow-fluid problems. With CFD analysis any engineering problem has a basic methodology; understanding flow model that consists of physical interactions and flow separations; proving model assumptions that consist of validating experimental results, and structural simulation model optimising which consists of decreasing pressure drop, laminar and turbulent mixing improvement, (Bakker, 2001). Without flow-fluid simulations it would be very difficult for meteorologists to calculate weather temperature, forecast the weather and announce natural disasters. It would be difficult for designers to improve the aerodynamic characteristics of a vehicle and gas engineers would not be able to obtain optimal pipe network designs. The numerical simulation has played a significant role in the engineering advancement since it has its own experimental and analytical knowledge of the engineering and numerical analysis (Bakker, 2001). It is obvious when considering the advances in mechanical engineering application that numerical simulation has major contributions by providing combination of theoretical and experimental analysis. Moreover, numerical simulation has also shown its ability to handle the governing equations and obtain the physical details of the problem formulation. Supporting experiments, extending the analytical solutions range and contribution in product development are key behind the numerical simulation successes over the last 30 years. Many applications of numerical simulation have been perceived in wind tunnel and combustion studies (Aman, 2018). The increase in the cost of experiments compared to the decrease of combustion cost

has forced the numerical simulation to be the best available alternative (Aman, 2018). To calculate the aerodynamic characteristics of any new design, a numerical simulation application is the cheapest and most accurate tool compared to the carried-out measuring in a wind tunnel and especially difficult conditions such as high temperature, toxic substances, large sizes that are not possible to conduct in wind experiments can be simulated using the numerical method with positive reliability (Aman, 2018).

2.1 Geometry shape and measures justification

- The simplified geometry illustrated below was selected following the supervisor advice as this shape is simple and has no complex features that would provide better explanation of the flow distribution problem.
- The idea is to understand flow non-uniformity for a basic shape and measure so the outcomes can lead to better analysation and then apply outcomes on complex geometries and designs.
- 10 outlets will be symmetrically designed to create a clear overall image of the flow distribution inside the duct.
- The only difference between the two geometries is the outlet size, reducing outlets has been conducted to observe the overall effect on flow non-uniformity.
- The reduction ratio is 1:4 as design 1 outlet width is 100mm and design 2 width is 25mm as shown in figure 4 and 5. All design modifications are conducted in line with supervisor advice.

2.1.1 CAD model

The two duct designs illustrated below will be simulated. SOLIDWORKS package was the selected tool to create the CAD model because of its accuracy and flexibility with ANSYS when it comes to modelling and importing. Two separate models were created as one solid part since assemblies are not acceptable and must be avoided to allow the simulation to run smoothly and obtain reliable results. The duct has been designed in 1:1 scale so actual dimension was used, and good reliability results are expected. Both model are fully defined.

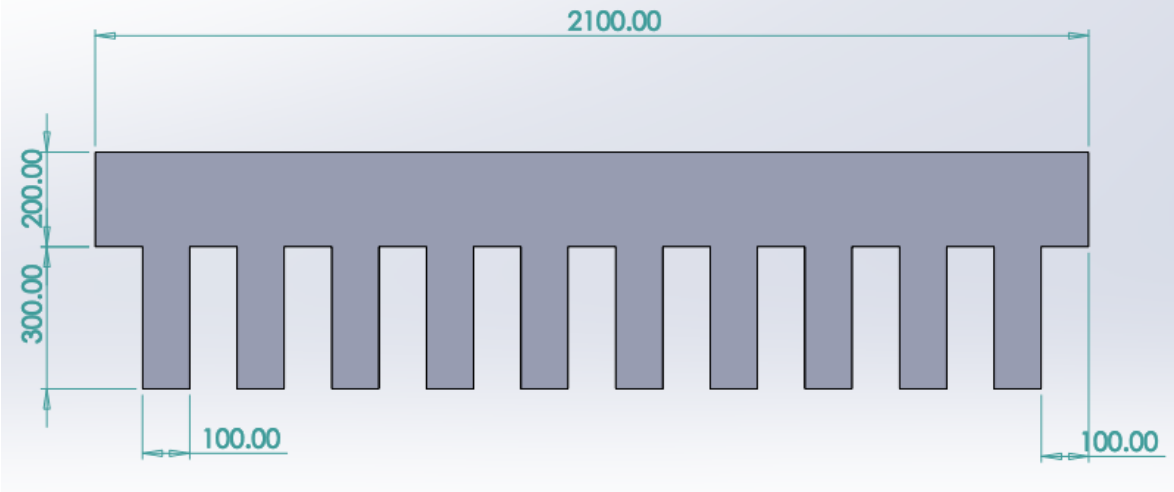

Figure 4: Design 1 side view (SolidWorks,2020)

Figure 5: Design 2 side view (SolidWorks,2020)

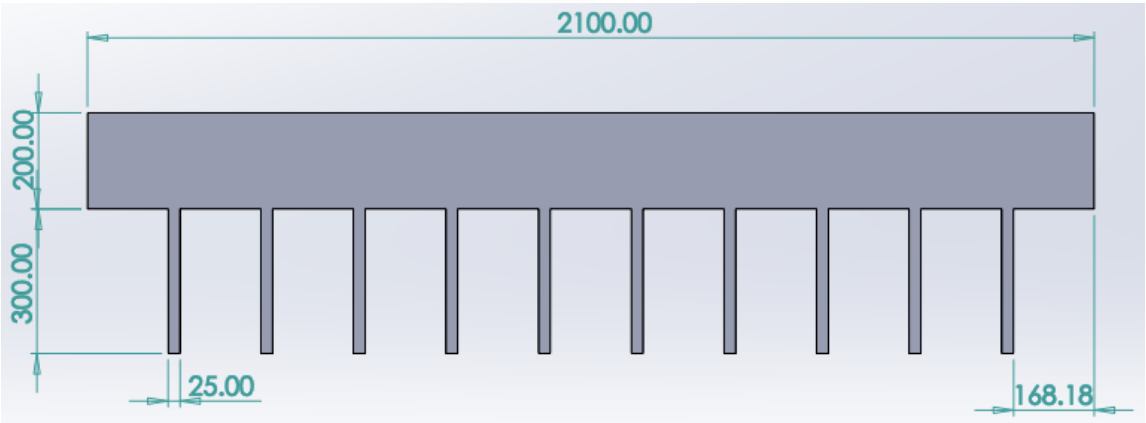

168.18mm is the distance between the last outlet and the wall and it's obvious that reducing outlet size has led to larger distance between outlets. All dimensions are in mm

Both designs will be used in the simulations to help understand the geometrical effects towards flow distribution and whether it increases or decreases uniformity inside the duct. Only one change was added to design 1 which is the outlets width as it was reduced from 0.1m to 0.025m. The area ratio for the two models was calculated using the following equation:

- $A.R.1 = N.\left(\frac{dh}{Dh}\right)^2 = 10.\left(\frac{0.133}{0.200}\right)^2 = 4.422$ $A.R.2 = 10.\left(\frac{0.044}{0.200}\right)^2 = 0.484$

Equation 7: Area Ratio Equation (Makky, 2021)

The above calculations show the area ratio for both geometries and how outlet reduction affect it. Both models were extruded using extruded boss/base feature for 0.2m after defining the model with all needed dimensions. The CAD models have been created in a simple procedure as this will simplify the entire problem for the next chapters. 3D view of the duct is presented below which shows both x and y axis.

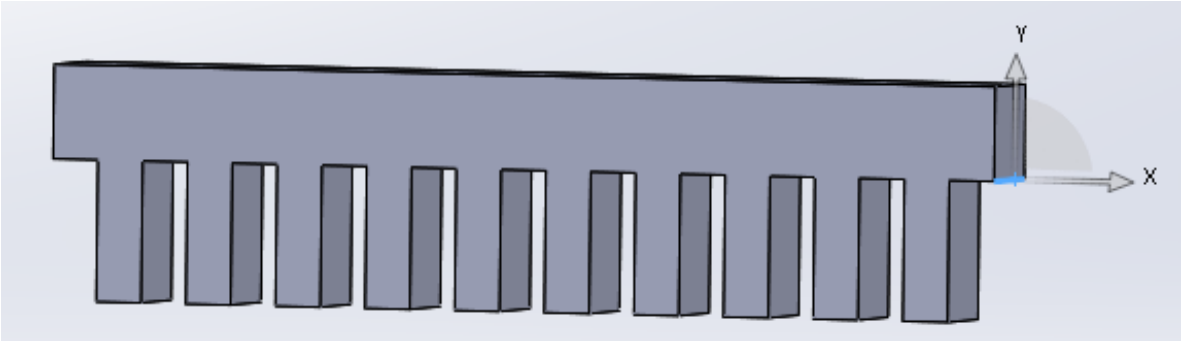

Figure 6: 3D view of the duct (SolidWorks,2020)

The models were imported to ANSYS Workbench CFX Package to initiate the simulations. Figure 7 illustrates how each selection was named according to its location and function.

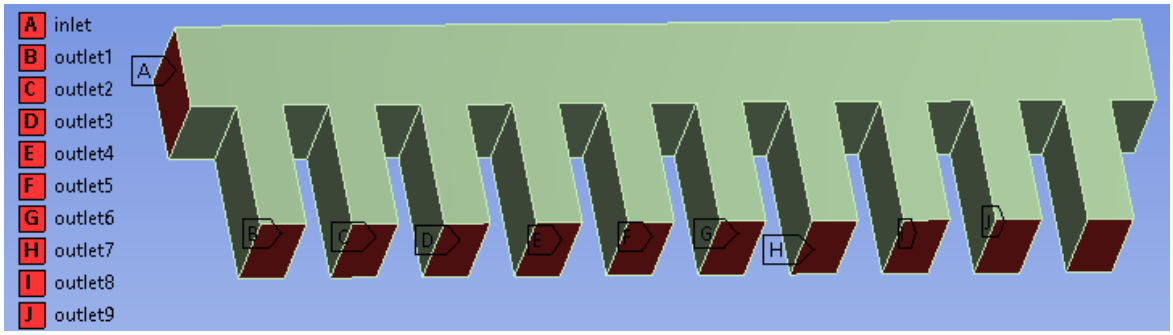

Figure 7: Named Selections Feature (Ansys workbench,2020)

2.2 Mesh Sensitivity Analysis

It is important to use the most sufficient refined mesh to ensure that the simulation results are as accurate as possible. Coarse meshes can lead to inaccurate results where analysis would be incorrect. Increasing the mesh density would force the model numerical solution to tend towards a unique value. As the mesh is refined, the computer resources increase

2.2.1 Possible Numerical Errors

Errors can be classified into two main categories:

- Acknowledged error which consists of physical approximation, computer round-off error, iterative independence error and discretisation error.
- Unacknowledged inaccuracy which refers to computer programming and user errors.

2.2.2 Physical approximation

The uncertainty in formulating and deliberating simplifications of the model cause physical approximation error. The continuum model is the only model that deals with these errors. Choosing the right governing equations is vital when it comes to the modelling errors for both solids and fluids. Modelling errors are linked with the issue of presenting a well-posed problem. Normally, turbulence quantities, transition and boundary conditions are required by modelling. Though some physical process is provided with high level of accuracy, the convenience of an efficient computation for the CFD code is required using simplified model. Conducting validation studies to examine the physical modelling errors is essential for certain models such as turbulent boundary layers, gas flows and inviscid flow.

2.2.3 Turbulence error

The selection of the most suitable turbulence model is a very important factor for the accuracy of the produced results using CFD analysis. To select the right turbulence model there are several factors which must be considered as each model has different set of boundary conditions that can affect the analysis. It has been noticed that most researchers tend to use RANS and K-Ɛ due to the simplicity of understanding it. However, there is an average of 25% error in results obtained by RANS turbulence model (W. Slater, 2020).

2.2.4 Computer Round-Off Error

Round off errors are considered to be much greater than other errors as they develop once the floating-point numbers are represented on the computer and the accuracy of storing numbers, nowadays with the introduction of computers they are stored with 32 or 64 bits. Once the round-off error is consideredas significant a test will be carried out running the code at higher precision with a computer that stores floating numbers at a greater precision. Even though it may not be possible for some complex algorithms, it can contribute to iterating a coarse grid solution towards zero residual machine. (W. Slater, 2020).

2.2.5 Iterative Convergence Error

For steady-state or unsteady problem, Iterative convergence is the required number of iterations to achieve residuals that are sufficiently close to zero. (Jiyuan Tu, 2018). This type of error normally shows up as result of the used iterative method where the simulation eventually has a stopping point. At the end of the simulations, the error scales to the variation in the solution. (W. Slater, 2020).

2.2.6 Discretization Errors

These are errors that are represented as algebraic expressions by the equations of flow governing and some different physical models in a domain of space and time (finite-element, volume, and difference). The mesh or grid is also known as the discrete spatial domain. The time step taken leads to the temporal discreteness to be manifested. The numerical error is also known as discretisation error. Once the grid points number rises and the grid spacing size is close to zero, the continuum representation of zero discretisation will be approached with a consistent numerical method. The solution tends to be less sensitive to the grid spacing and the continuum solution is approached once the mesh is refined, this is known as grids convergence. To determine the discretization error level that exists in a CFD simulation, the grid convergence is a very useful procedure. These errors, dependant on the grid size, are also known as discretisation error as they vanish when the grid size approaches zero. When it comes to conducting a CFD simulation the discretisation error is of most concern as it depends on the quality of the grid. On the other hand, it is usually difficult to accurately demonstrate the relationship between the grid quality and the accuracy of the solution before initiating the simulation. There are several steps that must be taken into consideration before generating the grid, such as boundary interfaces, resolution, density, aspect ratio, grid singularities and stretching. The flow feature also affects the discretisation level when it is resolved by the grid. The development of an error can also be a result of discontinuity such as shock, slip surfaces or interfaces. When the solution of a zone is approximated on the boundary of another zone this is known as interpolation error. (W. Slater, 2020).

These are errors that are represented as algebraic expressions by the equations of flow governing and some different physical models in a domain of space and time (finite-element, volume, and difference). The mesh or grid is also known as the discrete spatial domain. The time step taken leads to the temporal discreteness to be manifested. The numerical error is also known as discretisation error. Once the grid points number rises and the grid spacing size is close to zero, the continuum

representation of zero discretisation will be approached with a consistent numerical method. The solution tends to be less sensitive to the grid spacing and the continuum solution is approached once the mesh is refined, this is known as grids convergence. To determine the discretization error level that exists in a CFD simulation, the grid convergence is a very useful procedure. These errors, dependant on the grid size, are also known as discretisation error as they vanish when the grid size approaches zero. When it comes to conducting a CFD simulation the discretisation error is of most concern as it depends on the quality of the grid. On the other hand, it is usually difficult to accurately demonstrate the relationship between the grid quality and the accuracy of the solution before initiating the simulation. There are several steps that must be taken into consideration before generating the grid, such as boundary interfaces, resolution, density, aspect ratio, grid singularities and stretching. The flow feature also affects the discretisation level when it is resolved by the grid. The development of an error can also be a result of discontinuity such as shock, slip surfaces or interfaces. When the solution of a zone is approximated on the boundary of another zone this is known as interpolation error. (W. Slater, 2020).

2.2.7 Truncation Error

There is a difference between partial differential equation and the finite equation that is known as truncation error. It is also a function of the flow gradient and grid quality. The oscillations of a solution are often caused by the dispersive error; however, this can be fixed by the addition of artificial dissipation in order to reduce the size of the dispersive error. Dissipation error can result in gradients smoothing but comparing the dissipation level to the physical viscosity can contribute to contamination of the solution. The truncation error may face expansion as it is not used in the discretised equation. Once the leading order of the truncation error is second order, the numerical viscosity is represented by (dimension of length) ^2 / time), that is known as kinematic viscosity dimensions. Errors will be dampened if the vicious term is positive, and errors will grow if the viscous

term is negative. Iterative convergence is when the solution is not provided with proper convergence with respect to the steady-state solution or time step. (W. Slater, 2020).

2.2.8 Usage Errors

Usage errors normally show up because of improper use of the application. They tend to be present as discretisation and modelling errors. The accuracy of the simulation is established through models, grid, algorithm and inputs that are set by the user. An attempt to compute a turbulent flow with an assumption of inviscid flow can result in blatant errors. Even though the solution can be converged, the simulation conclusions would be sometimes incorrect. The errors may not be as obvious as proper turbulence model parameters selected for separated flows as the available options increase in a CFD code as the possibility of usage errors increases. The increased level options available in a CFD code increase the potential of usage error. Proper training and more experience with the software can minimise usage errors. Since less accuracy can be accepted at the conceptual stage the user may take the discretisation and modelling error as an attempt to conduct the simulation at the expense of accuracy. Usage errors may exist at the stage of CAD model, grid generation, and post-processing software. (W. Slater, 2020).

2.3 Mesh Study 1

A study of mesh convergence was carried out in order to identify the most suitable mesh size that will be used to measure the mass flow distribution at the outlets. The analysis study started with 0.016m for Max Tet size and 0.008m Min size and the number of elements was increased from 289725 to 4449312 elements over 6 studies which has been obtained by doubling the mesh size before every simulation.

Study No	Mesh 1	Mesh 2	Mesh 3	Mesh 4	Mesh 5	Mesh 6
Max Tet size (m)	0.016	0.012	0.010	0.008	0.0064	0.0056
Min size (m)	0.008	0.006	0.005	0.004	0.0032	0.0028
Number of Elements	289725	664356	1152000	2250000	4449312	6530793
$\dot{m}_{Out1}$ (kg/s)	0.5580	0.4920	0.0411	0.3820	0.3260	0.3060
$\dot{m}_{Out2}$	0.2970	0.2680	0.2950	0.3140	0.2490	0.2700
$\dot{m}_{Out3}$	0.2750	0.3010	0.3070	0.3090	0.2680	0.3650
$\dot{m}_{Out4}$	0.3520	0.3840	0.3820	0.3900	0.4390	0.5230
$\dot{m}_{Out5}$	0.6780	0.8110	0.8800	0.9830	1.0500	0.9840
$\dot{m}_{Out6}$	0.2610	3.0000	3.1900	3.3700	3.3900	3.2200
$\dot{m}_{Out7}$	0.5480	5.5600	5.5800	5.6200	5.5200	5.5300
$\dot{m}_{Out8}$	0.8030	7.9700	7.8700	7.8300	7.6400	7.6200
$\dot{m}_{Out9}$	0.1010	9.8500	9.6800	9.5600	9.3000	9.2600
$\dot{m}_{Out10}$	0.1153	11.2440	11.2820	11.1240	11.6970	11.8000
Sum	39.909	39.88	39.871	39.882	39.879	39.8795
$\dot{m}_{in}$ (39.878) Mass imbalance	0.0777	0.0050	0.9388	0.0100	0.0025	0.0037

Table 1: Mesh Convergence Study 1(Flow Distribution at each outlet)

2.4 Mesh Study 2

The error percentage was the main factor used to find the most suitable mesh size as the lowest error percentage indicated the most accurate mesh size. Mesh 5 with 0.0064 Max Tet and 0.0032 Min size was selected to be the used mesh to carry out the simulation of mass flow distribution. The

Study No	Mesh 1	Mesh 2	Mesh 3	Mesh 4	Mesh 5	Mesh 6
Max Tet size (m)	0.016	0.012	0.010	0.008	0.0064	0.0050
Min size (m)	0.008	0.006	0.005	0.004	0.0032	0.0025
Number of Elements	192575	446622	792000	1538750	3081393	6336000
$\dot{m}_{Out1}$ Kg/s	2.7937	2.8458	2.8521	2.9088	2.9188	2.7937
$\dot{m}_{Out2}$	3.1824	3.2429	3.2495	3.2897	3.2996	3.1824
$\dot{m}_{Out3}$	3.5579	3.5916	3.5880	3.6035	3.6312	3.6592
$\dot{m}_{Out4}$	3.8888	3.9132	3.9031	3.9267	3.9349	3.9602
$\dot{m}_{Out5}$	4.1938	4.2024	4.1706	4.1875	4.1913	4.2176
$\dot{m}_{Out6}$	4.4022	4.3807	4.3690	4.3858	4.3885	4.4086
$\dot{m}_{Out7}$	4.5187	4.4998	4.4946	4.5049	4.5080	4.5245
$\dot{m}_{Out8}$	4.5645	4.5487	4.5537	4.5545	4.5594	4.5657
$\dot{m}_{Out9}$	4.4769	4.4358	4.4662	4.3767	4.3423	4.2438
$\dot{m}_{Out10}$	4.3011	4.2190	4.2332	4.1420	4.1061	4.0287
Sum	39.89	39.8799	39.88	39.8801	39.8798	39.8801
$\dot{m}_{in}$ (39.876) %Mass imbalance	0.010	0.0097	0.010	0.012	0.0095	0.012

Table 2: Mesh Convergence Study 2 (Flow Distribution at each outlet)

Mesh Study table and figure shows the produced results and how mesh 5 was selected accordingly. The presented figure below illustrates how results accuracy keeps improving by increasing the number of elements and reducing the mesh size. Mesh sensitivity analysis is an essential procedure to follow as it contributes directly toward the reliability of the experiment.

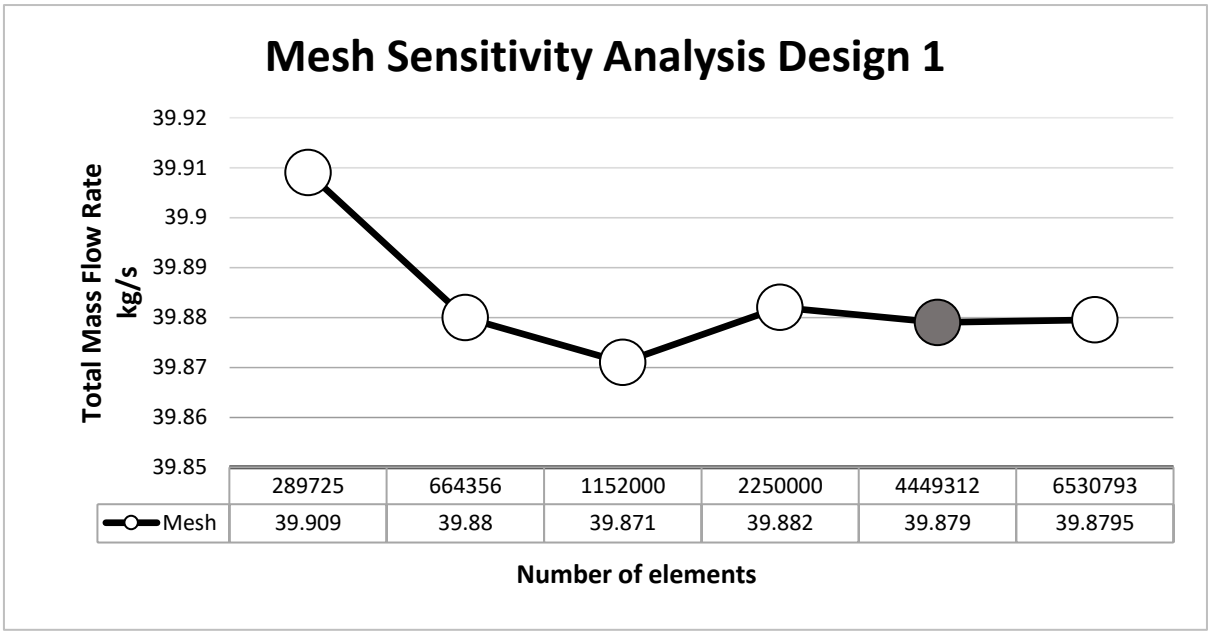

Figure 8: Mesh study Design 1 (Mass Flow Rate vs Number of elements)

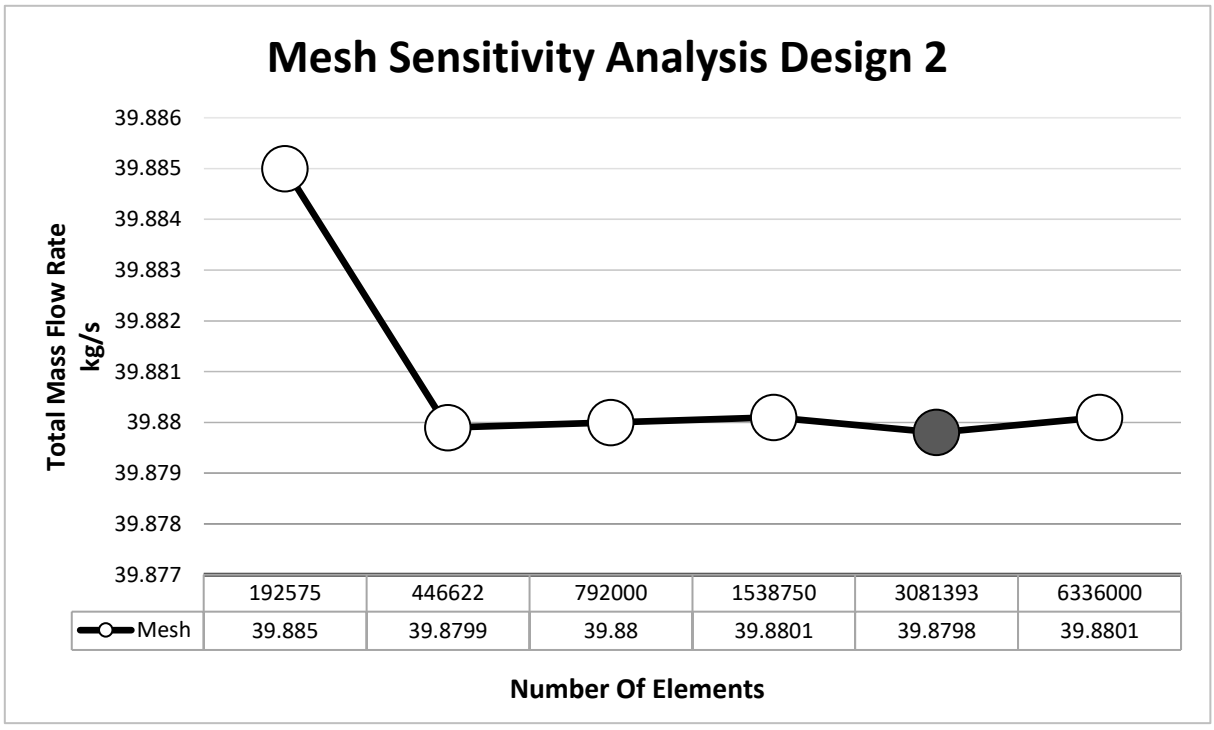

Figure 9: Mesh Study Design 2 (Mass Flow Rate vs Number of elements)

2.4.1 Mesh Quality

Skewness mesh metrics spectrum:

Excellent	Very good	Good	Acceptable	Bad	Unacceptable
0-0.25	0.25-0.50	0.50-0.80	0.80-0.94	0.95-0.97	0.98-1.00

Orthogonal Quality mesh metrics spectrum:

Unacceptable	Bad	Acceptable	Good	Very good	Excellent
0-0.001	0.001-0.14	0.15-0.20	0.20-0.69	0.70-0.95	0.95-1.00

Figure 10: Mesh Quality Metrics Skewness and Orthogonal. (ANSYS,2015)

The numerical simulations quality depends on mesh quality, poor mesh leads to inaccurate results. Thus, ensuring high quality mesh is required to produce reliable results. The carried-out mesh sensitivity analysis is an essential way to select the most suitable mesh. Additionally, ANSYS provide several tools to quantify mesh quality during and after mesh generation phase. Skewness and Orthogonal Quality are two of the most used metrics to verify mesh quality. Low orthogonal and high skewness values are not recommended. It is required to ensure minimum orthogonal quality > 0.15 and maximum skewness < 0.94.

Design 1	Mesh 1	Mesh 2	Mesh 3	Mesh 4	Mesh 5	Mesh 6
Skewness (Avg)	0.01066	0.00391	0.02846	0.00205	1.3074e-010	1.3074e-010
Orthogonal (Avg)	0.9997	0.9995	0.99992	0.99995	1	1

Table 3: Mesh Quality Metrics for Design 1 (ANSYS, 2021)

Design 2	Mesh 1	Mesh 2	Mesh 3	Mesh 4	Mesh 5	Mesh 6
Skewness (Avg)	0.00584	0.004524	0.006024	0.00329	0.00098	0.001613
Orthogonal (Avg)	0.99993	0.99996	0.99992	0.99998	0.99999	0.99998

Table 4: Mesh Quality Metrics for Design 2 (ANSYS, 2021)

Mesh Metric	Orthogonal Quality	Mesh Metric	Skewness
Min	1.	Min	1.3057e-010
Max	1.	Max	1.3311e-010
Average	1.	Average	1.3074e-010

Figure 11: Mesh 5 Orthogonal quality and Skewness Design 1 (ANSYS, 2021)

2.4.2 Mesh Selection Justification

Mesh 5 was chosen for design 1 and 2 simulations. It was selected as this mesh produces less grid convergence percentage. The idea was to create a fully-defined and simplified geometry to ensure high mesh quality. Both geometries were solid with no complex features such as intersections or sharp outcroppings. A simplified geometry that is enclosed means clean mesh and no geometrical defects. Mesh 5 was the most suitable because it led to the lowest skewness ratio maintaining an overall grid. Table 3 ,4 and figure 11 show mesh quality metrics from mesh 1 to mesh 6. It is obvious that reducing the mesh size led to excellent mesh quality as presented in figure 10. For the skewness value mesh 5 alongside mesh 6 produced the lowest value which is adequate for the simulation purposes. Orthogonal quality values continued to increase as mesh size decreases, and from figure 10 orthogonal quality values approach 1 as the mesh quality improve. Taking simulation time consuming into consideration and according to the provided information in table 3 and 4, mesh 5 is the most suitable for the simulation purposes.

2.5 CFD Approach

This section will be comprised of explanation and justification of the selected boundary conditions and parameters using CFX ANSYS package. The dimension of the model is confirmed and ready to be simulated. The speed of the flow at the inlet has been set to (1 m/s) which will be increased by 1m/s after each simulation to observe mass flow rate effect on flow distribution. The air temperature was set to 18ºC. Table 5 below shows the simulation properties and boundary conditions.

Model(s)	Viscous (K-epsilon)
Domain Type	Fluid Domain
Assumption	3D Steady fluid flow, Incompressible flow, and fully developed flow at the inlet.
Materials	Fluids (water)-Continuous Fluid Density 998.2 kg/m^3 viscosity 0.001003 kg / (m.s)
Location	Boundary condition
Inlet	Flow Regime: Subsonic Mass and Momentum: normal speed Normal Speed: 1-10 m/s
Outlet 1-10	Flow Regime: Subsonic Mass and Momentum: average static pressure Relative Pressure: 0 Pa Pressure average over whole outlet
Right & Left Side Wall	Mass and Momentum: Free slip Wall

Table 5: Simulation Parameters (Ansys, 2021)

2.6 ANSYS Simulation

After selecting the suitable mesh both designs are ready to be simulated, in this section a full procedure will be described. All simulations have the same exact procedure with one minor adjustment which is inlet mass flow rate. A CFX Ansys analysis has been conducted to compute this model that is imported from SolidWorks.

Using the named selection feature the next stage is to name the model faces each according to its location and purpose. There is a link between this stage and the setup stage where boundary condition can be applied. However, it is essential to mention that any error at this stage would lead to an error at the next stages.

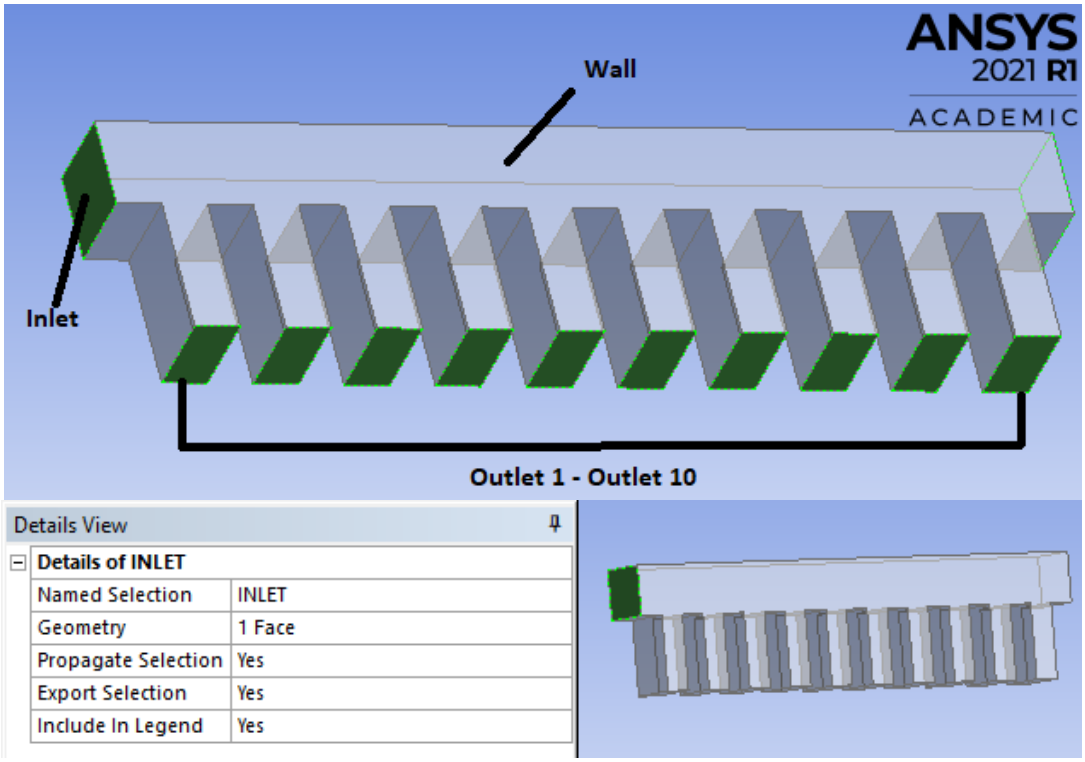

Figure 12: Naming Faces using Named selection Feature (Ansys, 2021)

Meshing is the simulation third stage. This stage can be conducted after successfully naming all model faces. The mesh convergence study and mesh quality stage successfully confirmed the suitable mesh size that will ensure good results reliability. Figure below illustrates mesh properties and statistics that used to set up the simulation.

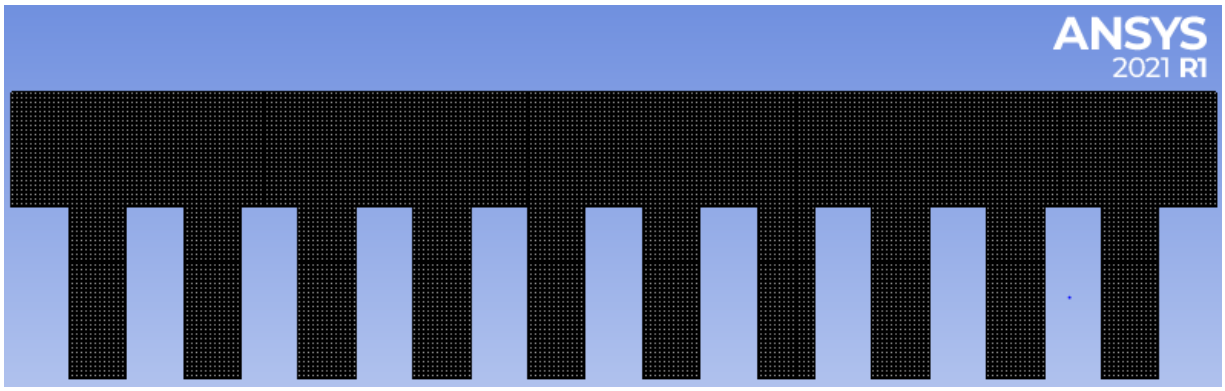

Details of "Mesh"

Curvature Min Size	Default (3.2e-005...
Curvature Normal Angle	Default (18.0°)
Capture Proximity	No
Bounding Box Diagonal	2.1679 m
Average Surface Area	7.7391e-002 m²
Minimum Edge Length	1.e-001 m
Quality	
Inflation	
Advanced	
Statistics	
Nodes	4614016
Elements	4437468

Figure 13: Creating Mesh using the Suitable Mesh Size (Ansys. 2021)

The next stage of the procedure is the set-up stage where boundary conditions are applied. As stated previously the temperature is 18ºC and the flow speed is 1 m/s . As presented in figure 14, different boundary conditions have been set to each face according to its location as mentioned before .

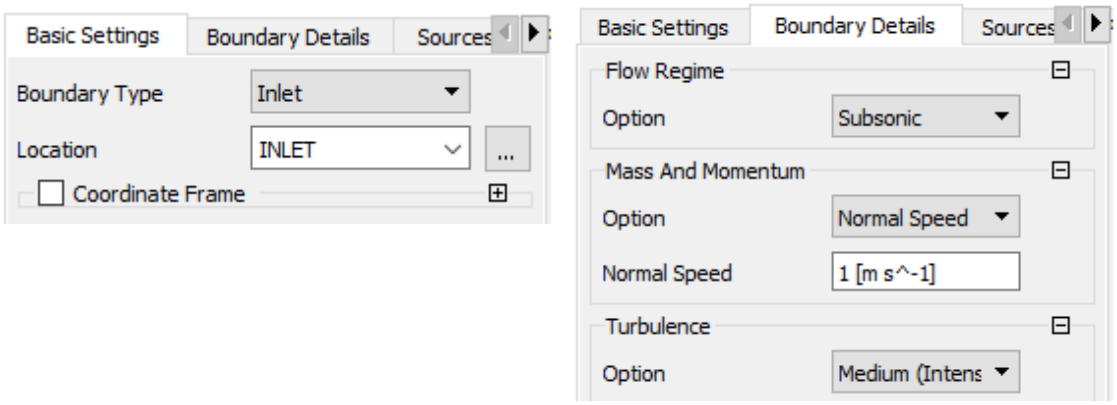

Figure 14: Applying Boundary conditions (Ansys, 2021)

The final stage is the iteration set-up stage, min iterations has been set to 1 and the maximum iterations number considering time taken were set to 1000 as shown below. The simulation can be run and converge successfully, and accurate results are expected.

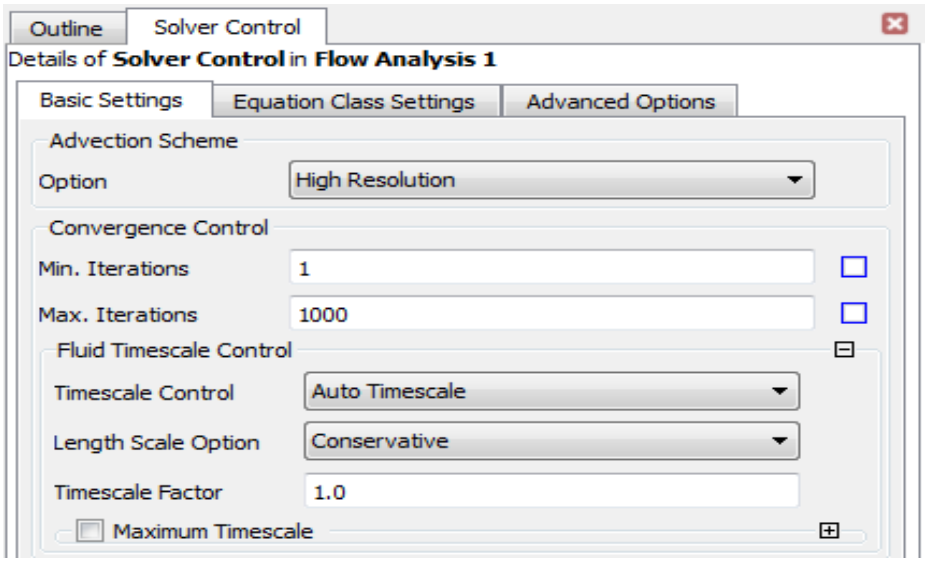

Figure 15: Iterations Number Set-Up (Ansys, 2021)

CHAPTER THREE

Results

3.1Simulation (1m/s Inlet Flow Velocity)

The presented table below shows the results of the first simulation with 1 m/s flow velocity at the inlet.

Location	Outlet1	Outlet2	Outlet3	Outlet4	Outlet5	Outlet6	Outlet7	Outlet8	Outlet9	Outlet10
Mass Flow Design 1 (kg/s)	0.326	0.249	0.268	0.439	1.05	3.39	5.52	7.64	9.30	11.7
Distribution	0.817%	0.624%	0.672%	1.103%	2.633%	8.501%	13.84%	19.15%	23.32%	29.34%
Mass Flow Design 2 (kg/s)	2.9133	3.2943	3.6258	3.9299	4.1867	4.3848	4.5053	4.5581	4.3577	4.1241
Distribution	7.306%	8.262%	9.094%	9.856%	10.50%	10.99%	11.29%	11.43%	10.92%	10.34

Table 6: Flow Distribution Simulation Results Design 1 vs Design 2

The figure below shows flow distribution percentage for design 1 and 2. The significant difference between both lines indicate how design affect flow distribution.

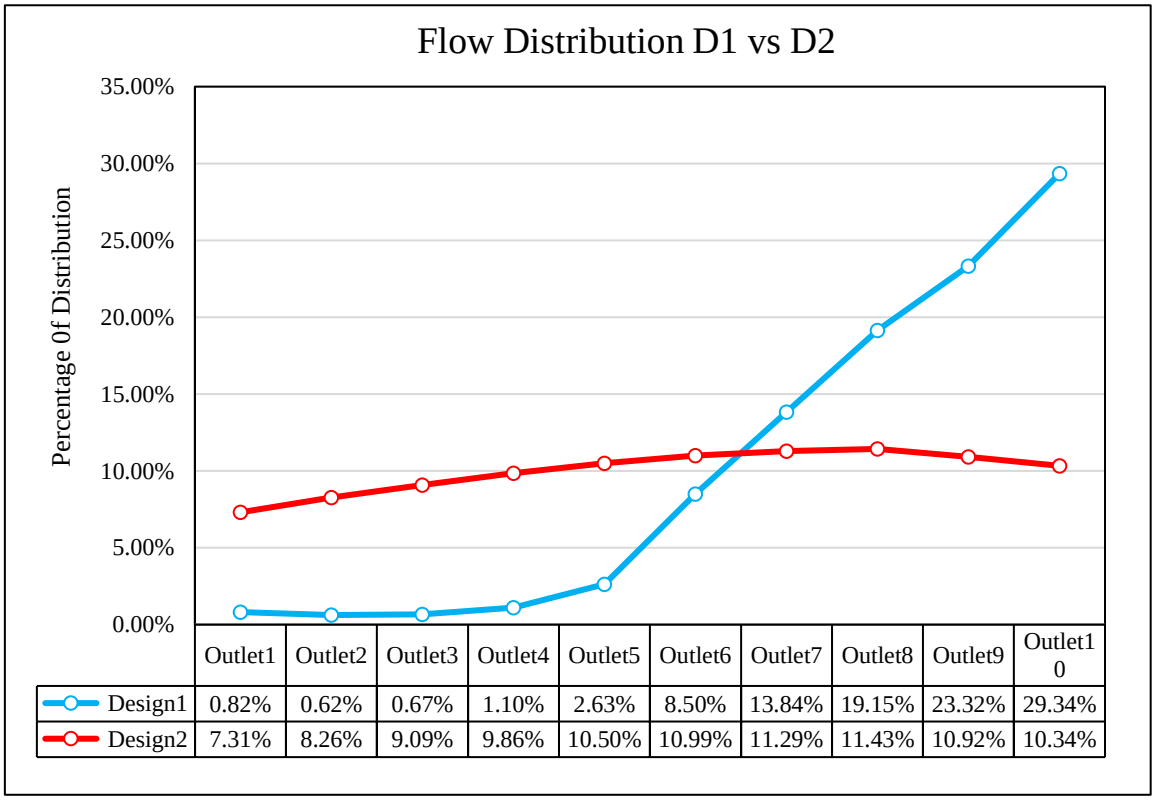

Figure 16: Mass Flow Distribution Line Design 1 vs Design 2

3.2 Simulation (2m/s Inlet Flow Velocity)

The presented table below shows the results of the first simulation with 2 m/s flow velocity at the inlet.

Location	Outlet1	Outlet2	Outlet3	Outlet4	Outlet5	Outlet6	Outlet7	Outlet8	Outlet9	Outlet10
Mass Flow Design 1 (kg/s)	0.700	0.535	0.505	0.757	2.010	6.770	11.10	15.54	19.02	22.94
Distribution%	0.877%	0.670%	0.633%	0.949%	2.520%	8.489%	13.91%	19.48%	23.85%	28.77%
Mass Flow Design 2 (kg/s)	5.7367	6.5081	7.182	7.8040	8.3357	8.7559	9.0213	9.1441	8.8804	8.3912
Distribution%	7.192%	8.159%	9.004%	9.784%	10.45%	10.97%	11.31%	11.46%	11.13%	10.52%

Table 7: Flow Distribution Simulation Results Design 1 vs Design 2

The figure below shows flow distribution percentage for design 1 and 2. The significant difference between both lines indicate how design affect flow distribution.

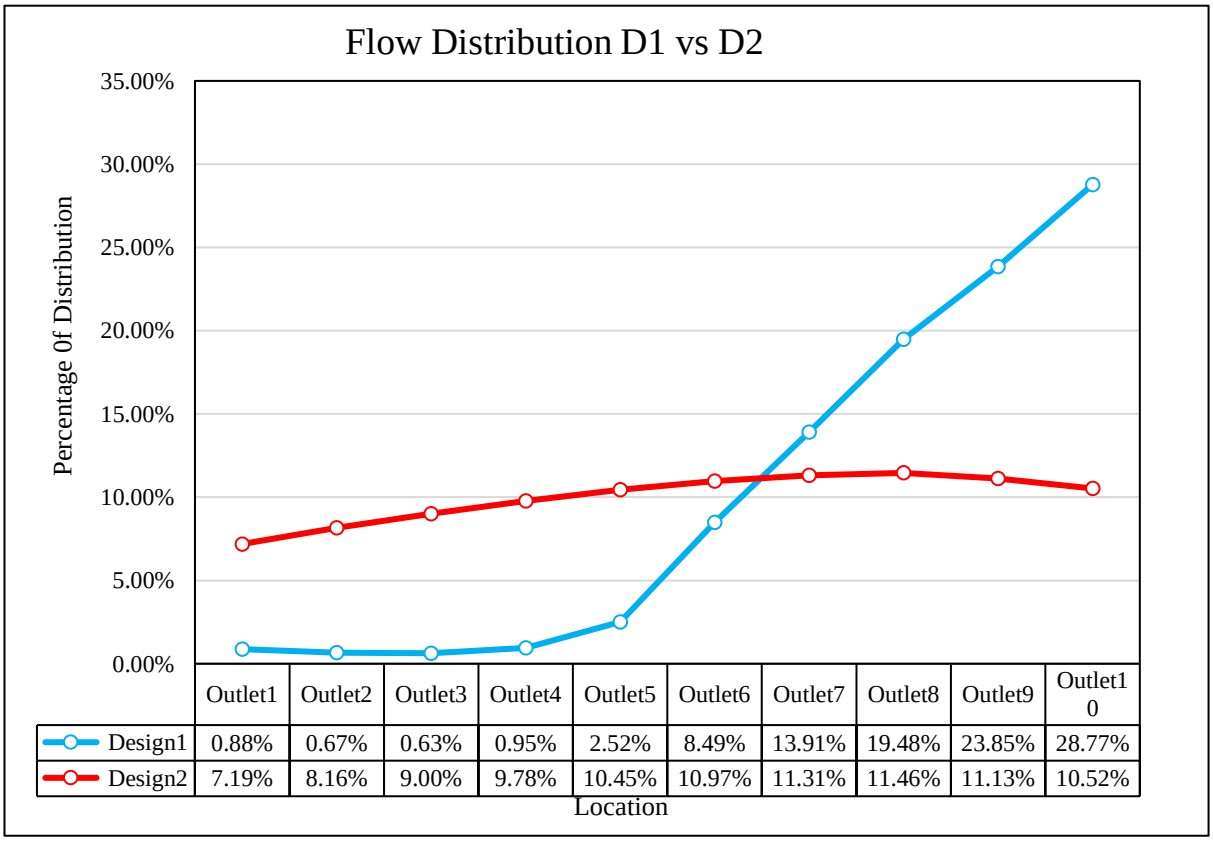

Figure 17: Mass Flow Distribution Line Design 1 vs Design 2

3.3 Simulation (2m/s Inlet Flow Velocity)

The presented table below shows the results of the first simulation with 3 m/s flow velocity at the inlet.

Location	Outlet1	Outlet2	Outlet3	Outlet4	Outlet5	Outlet6	Outlet7	Outlet8	Outlet9	Outlet10
Mass Flow Design 1 (kg/s)	1.0556	0.79900	0.74157	1.0763	2.8844	9.9952	16.498	23.217	28.744	34.628
Distribution%	0.882%	0.667%	0.619%	0.899%	2.410%	8.353%	13.78%	19.40%	24.02%	28.94%
Mass Flow Design 2 (kg/s)	8.5558	9.214	10.739	11.679	12.487	13.132	13.546	13.739	13.399	12.642
Distribution%	7.150%	7.700%	8.975%	9.761%	10.43%	10.97%	11.32%	11.48%	11.19%	10.56%

Table 8: Flow Distribution Simulation Results Design 1 vs Design 2

The figure below shows flow distribution percentage for design 1 and 2. The significant difference between both lines indicate how design affect flow distribution.

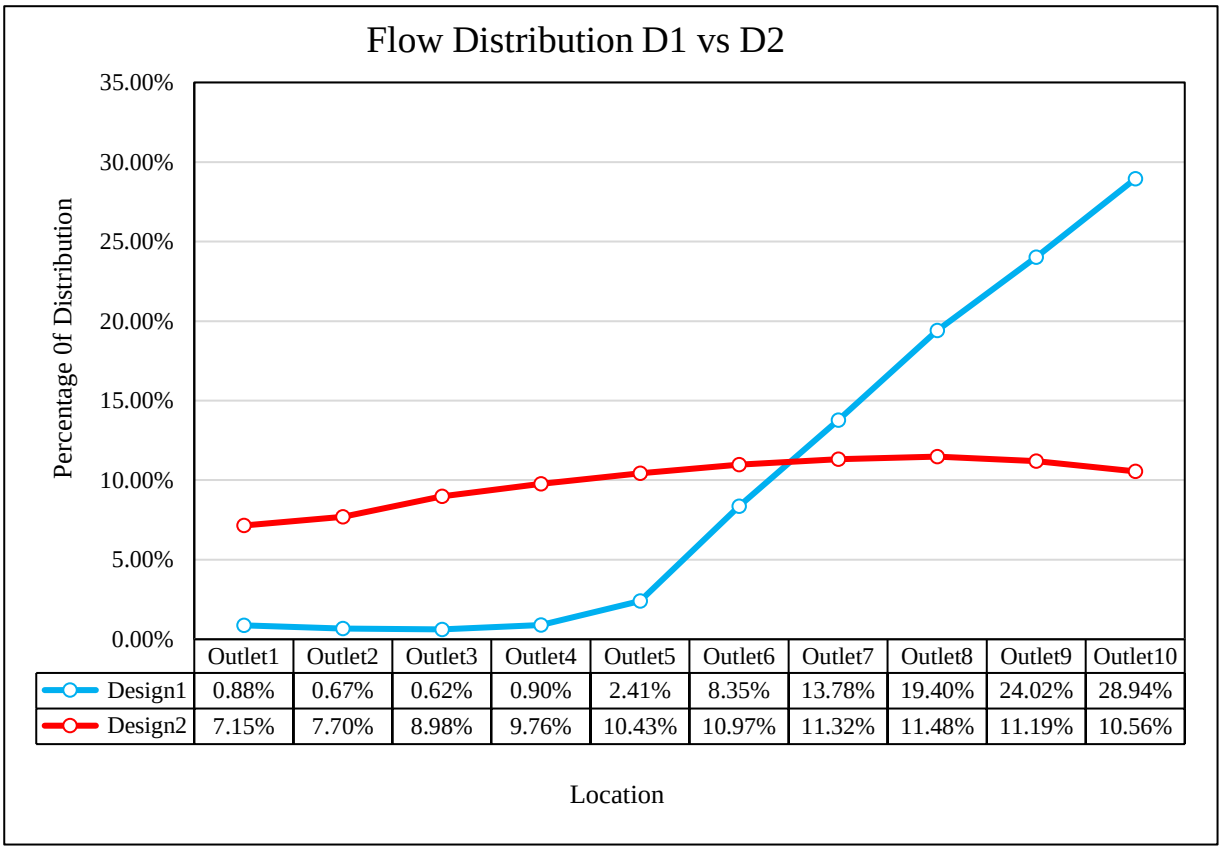

Figure 18: Mass Flow Distribution Line Design 1 vs Design 2

3.4 Simulation (4m/s Inlet Flow Velocity)

The presented table below shows the results of the first simulation with 4m/s flow velocity at the inlet.

Location	Outlet1	Outlet2	Outlet3	Outlet4	Outlet5	Outlet6	Outlet7	Outlet8	Outlet9	Outlet10
Mass Flow Design 1 (kg/s)	1.3897	1.0212	0.94194	1.4281	3.7380	13.115	21.821	30.859	38.393	46.810
Distribution%	0.871%	0.640%	0.590%	0.895%	2.343%	8.222%	13.68%	19.347%	24.07%	29.347%
Mass Flow Design 2 (kg/s)	11.363	12.925	14.286	15.546	16.63	17.505	18.070	18.338	17.933	16.923
Distribution%	7.124%	8.103%	8.956%	9.746%	10.42%	10.97%	11.33%	11.49%	11.24%	10.61%

Table 9: Flow Distribution Simulation Results Design 1 vs Design 2

The figure below shows flow distribution percentage for design 1 and 2. The significant difference between both lines indicate how design affect flow distribution.

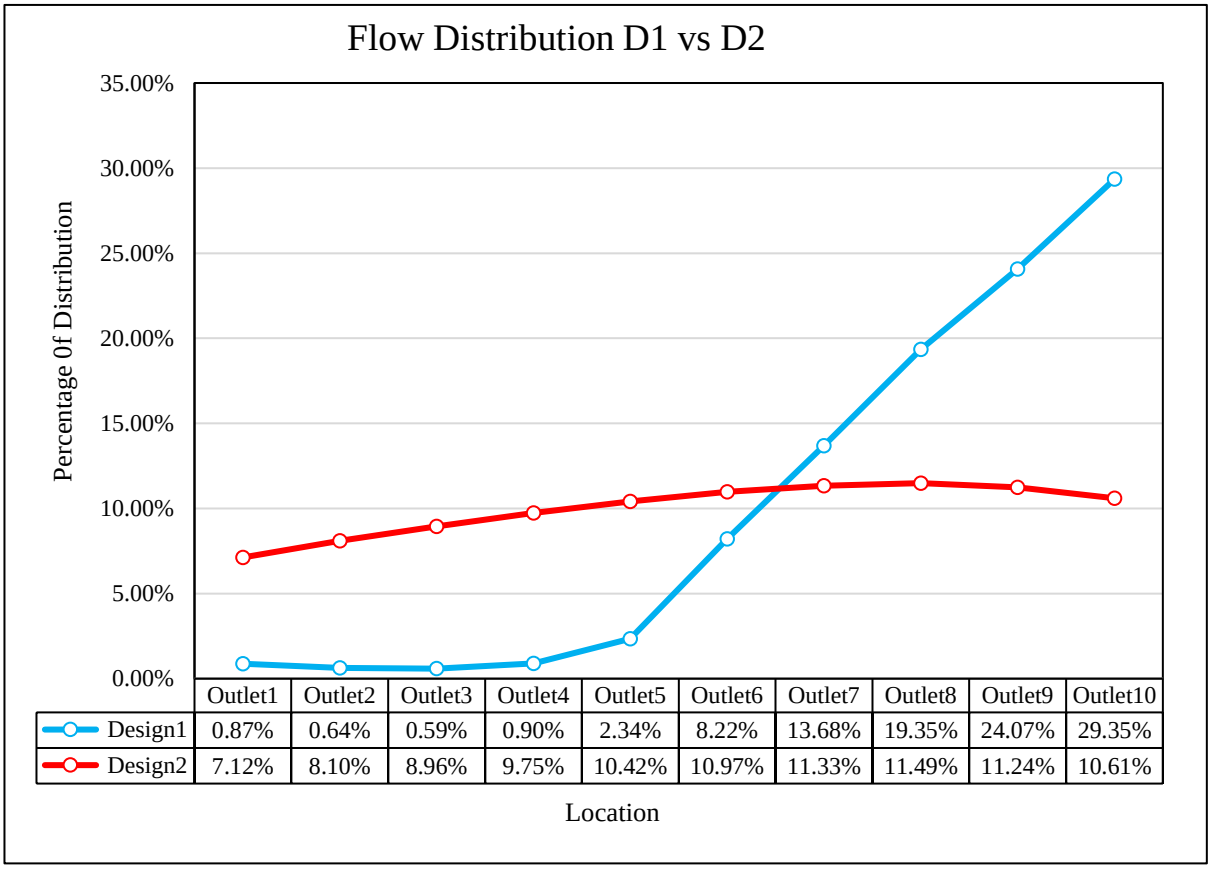

Figure 19: Mass Flow Distribution Line Design 1 vs Design 2

3.5 Simulation (5m/s Inlet Flow Velocity)

The presented table below shows the results of the first simulation with 5 m/s flow velocity at the inlet.

Location	Outlet1	Outlet2	Outlet3	Outlet4	Outlet5	Outlet6	Outlet7	Outlet8	Outlet9	Outlet10
Mass Flow Design 1 (kg/s)	1.6260	1.2124	1.1456	1.8008	4.6038	16.235	27.171	38.546	48.133	58.925
Distribution%	0.8155%	0.608%	0.590%	0.903%	2.309%	8.142%	13.62%	19.33%	24.14%	29.55%
Mass Flow Design 2 (kg/s)	14.155	16.119	17.826	19.406	20.77	21.876	22.598	22.942	22.475	21.233
Distribution%	7.097%	8.084%	8.940%	9.733%	10.41%	10.97%	11.33%	11.51%	11.27%	10.65%

Table 10: Flow Distribution Simulation Results Design 1 vs Design 2

The figure below shows flow distribution percentage for design 1 and 2. The significant difference between both lines indicate how design affect flow distribution.

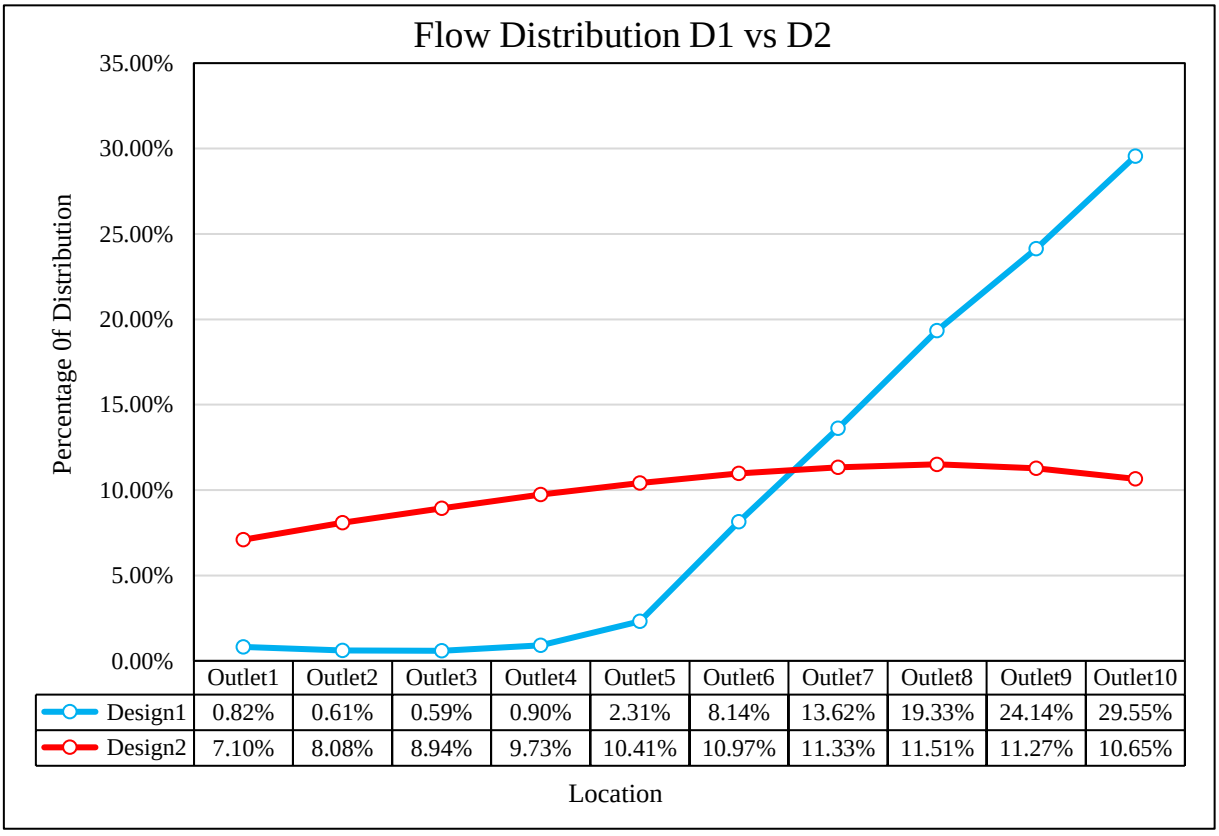

Figure 20: Mass Flow Distribution Line Design 1 vs Design 2

3.6 Reynolds Number Calculations

For many fluid flow situations, it is vital to predict flow patterns and Reynolds number (Re) helps to identify flow status. For low Reynold numbers, flows are identified as laminar flow ‘‘sheet-like’’. high Reynold numbers means turbulent flows are dominating.

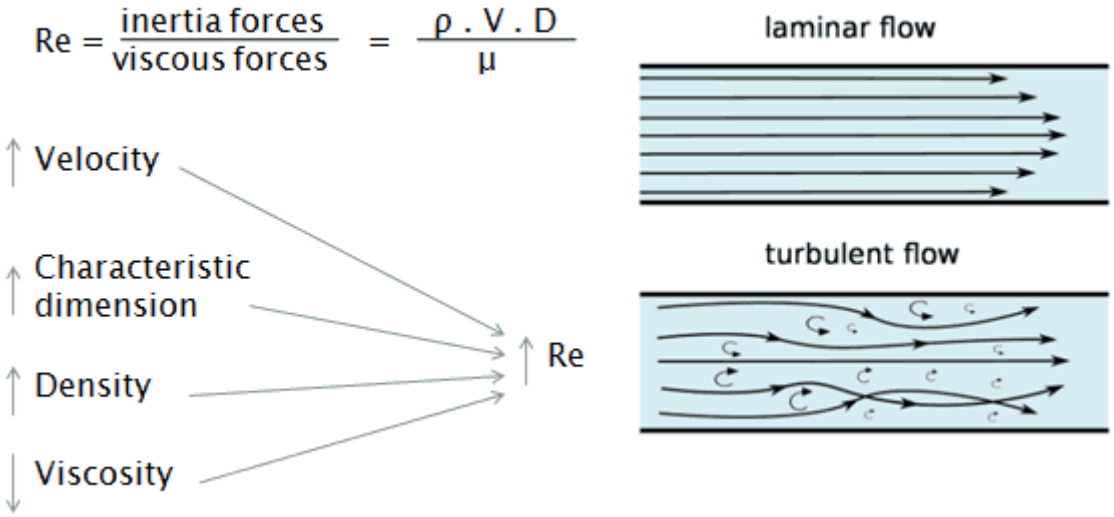

Figure 21: Reynold Number Flows (Hyper, 2021)

$$Re = \frac{\rho_{air} \times U \times l}{\mu_{air}}$$

Equation 8: Reynold Number Calculation

$$\mathrm{Re} = \frac{998 \times 1 \times 0.200}{0.0008900} =$$

The table below show the flow properties and status and it is obvious that the flow tends to be turbulent. Reynold number is unitless.

Flow velocity U	Mass flow(inlet)	ρ_{water}	Hydraulic diameter	μwater	Reynolds Number
1 m/s	39.87 kg/s	998 Kg/m	0.200 m^2	0.0008900 N. s/m^2	224269.66
2 m/s	79.75 kg/s	998 Kg/m	0.200 m^2	0.0008900 N. s/m^2	448539.3
3 m/s	119.65 kg/s	998 Kg/m	0.200 m^2	0.0008900 N. s/m^2	672809
4 m/s	159.5 kg/s	998 Kg/m	0.200 m^2	0.0008900 N. s/m^2	897078.6
5m/s	199.38 kg/s	998 Kg/m	0.200 m^2	0.0008900 N. s/m^2	1121348

Table 11: Reynold Numbers

CHAPTER FOUR

Research Findings

4.1 Flow Distribution Design 2

The following table and figure indicate the distributed fluid flow to each outlet inside Design 1 model at 5 different sets of inlet mass flow rate.

Velocity of Flow at inlet	1 m/s	2m./s	3m/s	4m/s	5m/s
Location/ Mass Flow Rate	39.87 Kg/s	79.748 Kg/s	119.65 Kg/s	159.5 Kg/s	199.38 Kg/s
Outlet1	0.326	0.700	1.056	1.389	1.626
Outlet2	0.249	0.535	0.799	1.021	1.212
Outlet3	0.268	0.505	0.743	0.942	1.145
Outlet4	0.439	0.757	1.076	1.4281	1.800
Outlet5	1.051	2.010	2.884	3.7380	4.603
Outlet6	3.392	6.770	9.995	13.115	16.235
Outlet7	5.521	11.103	16.495	21.821	27.171
Outlet8	7.644	15.543	23.217	30.859	38.546
Outlet9	9.302	19.022	28.744	38.393	48.133
Outlet10	11.712	22.941	34.628	46.810	58.925

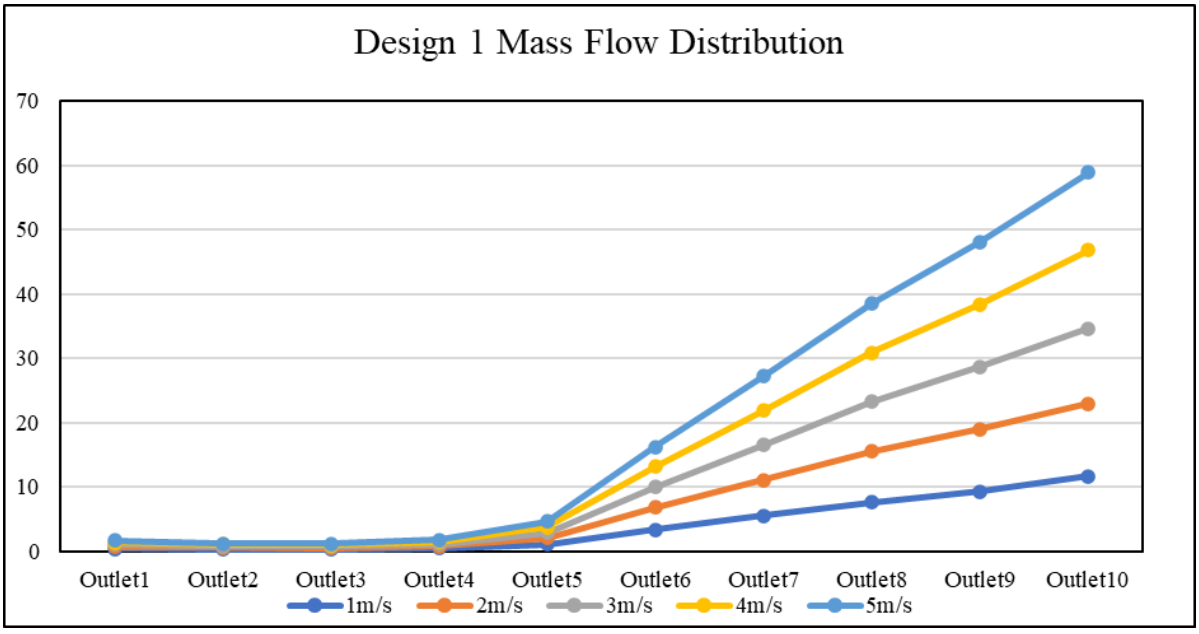

Figure 22: Design 1 Flow Distribution Line for 5 Inlet Flow Velocities

4.2 Flow Distribution Design 2

The following table and figure indicate how the flow is distributed to each outlet inside Design 2 model at 5 different sets of inlet mass flow rate.

Velocity of Flow at inlet	1 m/s	2m./s	3m/s	4m/s	5m/s
Location/ Mass Flow Rate	39.87 Kg/s	79.748 Kg/s	119.65 Kg/s	159.5 Kg/s	199.38 Kg/s
Outlet1	2.913	5.736	8.555	11.363	14.155
Outlet2	3.294	6.508	9.214	12.925	16.119
Outlet3	3.625	7.182	10.739	14.286	17.826
Outlet4	3.929	7.804	11.679	15.546	19.406
Outlet5	4.186	8.335	12.487	16.63	20.77
Outlet6	4.384	8.755	13.132	17.505	21.876
Outlet7	4.505	9.021	13.546	18.07	22.598
Outlet8	4.558	9.144	13.739	18.338	22.942
Outlet9	4.357	8.880	13.399	17.933	22.475
Outlet10	4.124	8.391	12.642	16.923	21.233

Table 13: Mass Flow Rate Distribution Results Design 2

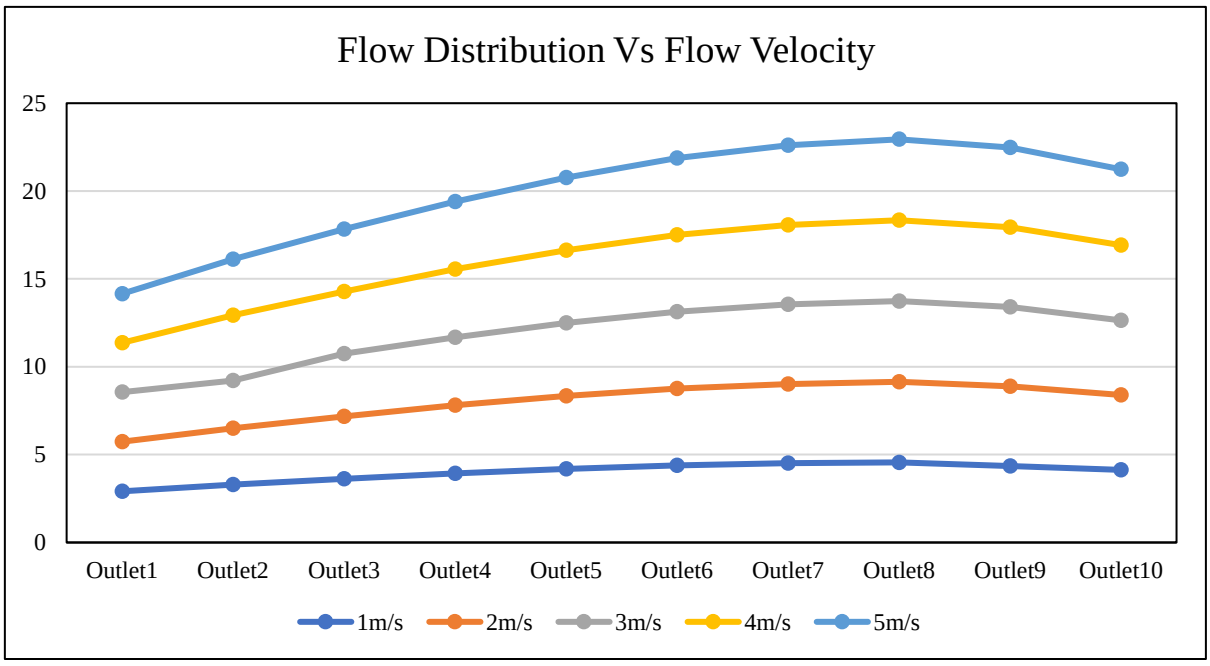

Figure 23: Design 2 Flow Distribution Line for 5 Inlet Flow Velocities

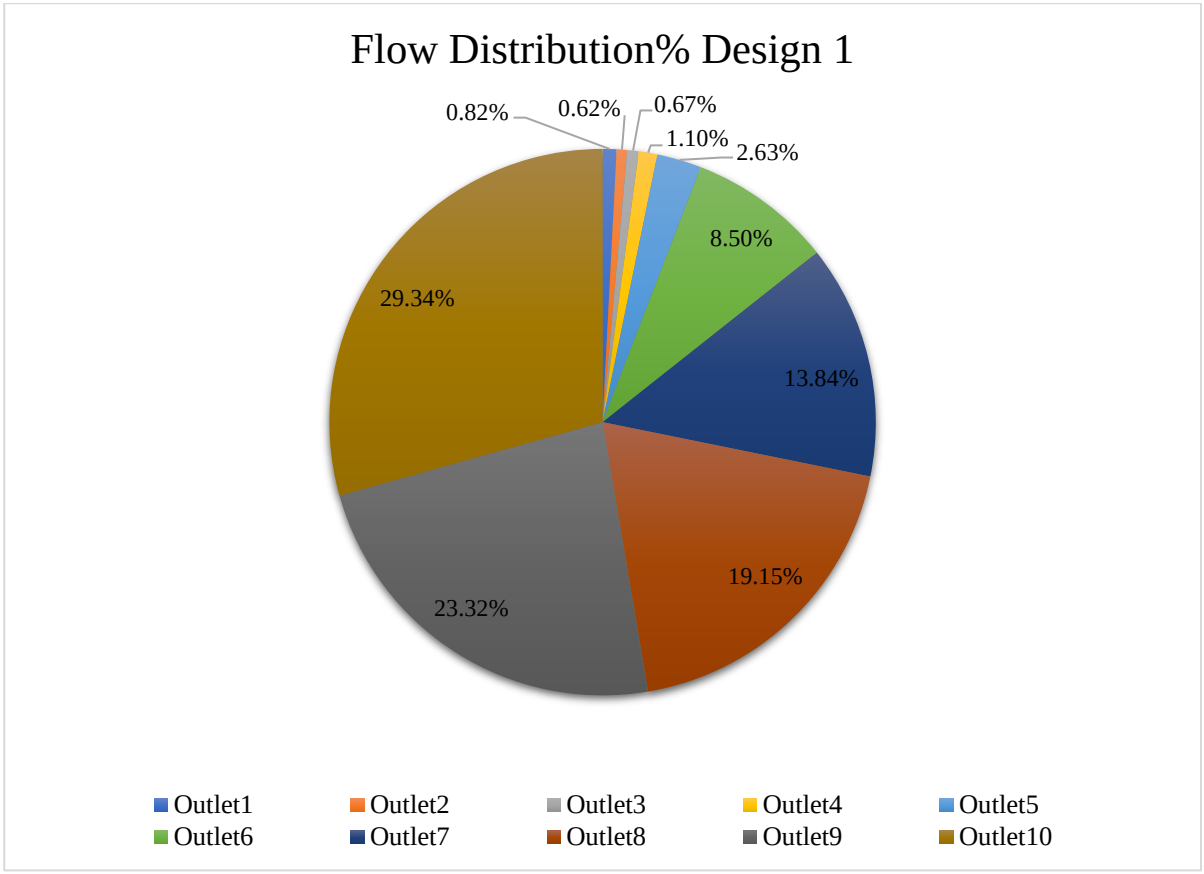

Figure 24: Flow Distribution Pie Design 1

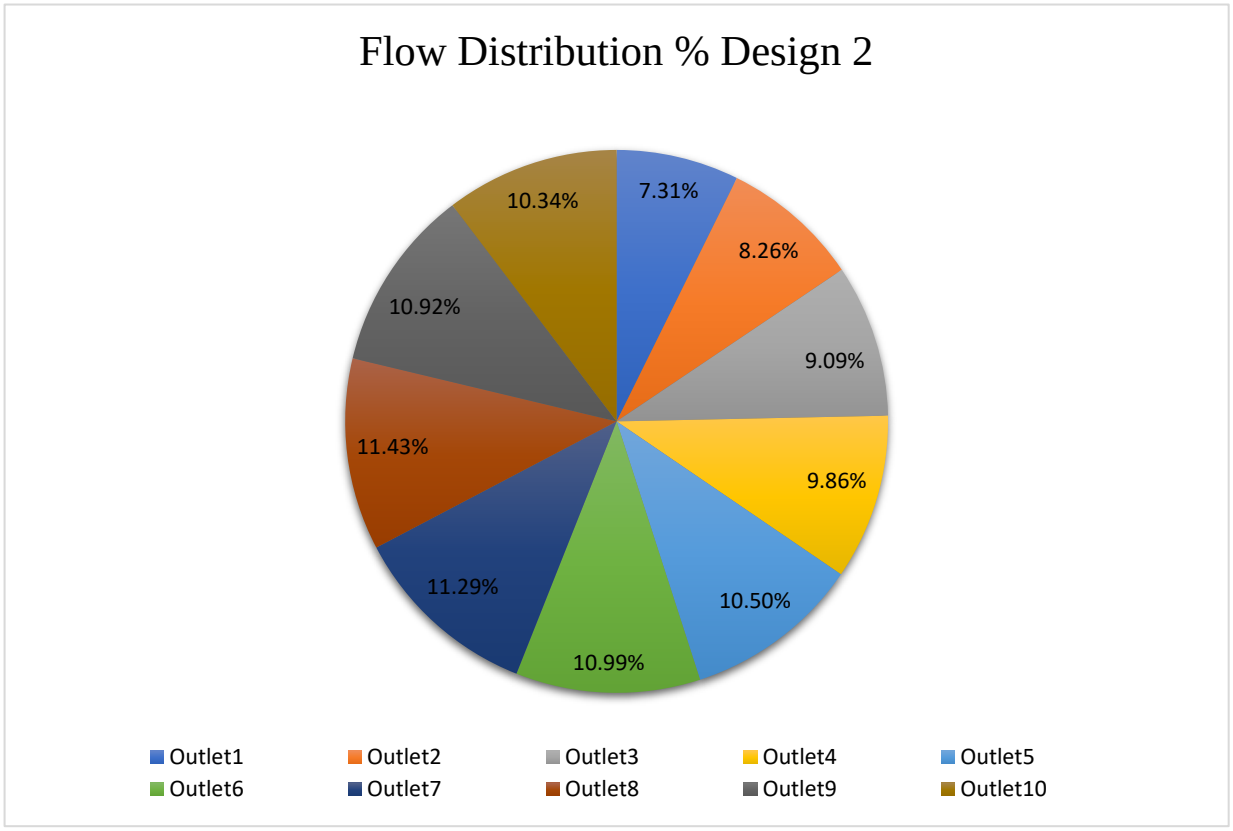

Figure 25: Flow Distribution Pie Design 2

4.3Non-Uniformity Coefficient Design 1(Φ)

It is vital to determine non-uniformity ecoefficiency to evaluate the flow inside any distribution system and to contribute towards achieving the optimal design. It is a dimensionless factor where large values represent less flow distribution inside the configuration. Lower value of non-uniformity ecoefficiency is key to obtaining the best possible design.

$$\varphi = \sqrt{\frac{\sum_{i=1}^{n} (\beta_i - \bar{\beta})^2}{N}} \qquad where, \quad \beta_i = \frac{Q_i}{Q} \quad ; \quad and, \quad \bar{\beta} = \frac{\sum_{i=0}^{n} \beta_i}{N}$$

The coefficient is calculated using the above equation for both designs at different inlet flow rates and this will provide a clear description of the design impact towards the flow distribution.

Inlet Flow Velocity	1 m/s	2 m/s	3 m/s	4 m/s	5 m/s
Mass Flow rate (Q) Kg/s	39.87	79.76	119.65	159.5	199.38
Boutlet1 (Q1/Q)	0.00817	0.00877	0.00882	0.00871	0.008155
Boutlet2 (Q2/Q)	0.00626	0.00670	0.00667	0.00640	0.00608
Boutlet3 (Q3/Q)	0.00672	0.00633	0.00619	0.00590	0.00590
Boutlet4 (Q4/Q)	0.01103	0.00949	0.00899	0.00895	0.00903
Boutlet5 (Q5/Q)	0.02633	0.02520	0.02411	0.02343	0.02309
Boutlet6 (Q6/Q)	0.08501	0.08489	0.08350	0.08222	0.08142
Boutlet7 (Q7/Q)	0.13841	0.13911	0.13780	0.13687	0.13621
Boutlet8 (Q8/Q)	0.19150	0.19480	0.19401	0.19345	0.19331
Boutlet9 (Q9/Q)	0.23321	0.23850	0.24020	0.24075	0.24142
Boutlet10 (Q10/Q)	0.29340	0.28770	0.28940	0.29354	0.29553
Non-Uniformity Coefficient ϕ design 1	0.10222	0.102345	0.102924	0.10379	0.10434

Table 14: Non-Uniformity Coefficient Design 1

4.4 Non-Uniformity Coefficient Design 2(Φ)

The coefficient was calculated using the provided equation which is indicated in the following table to discuss any difference that Design 2 can obtain.

Inlet Flow Velocity	1 m/s	2 m/s	3 m/s	4 m/s	5 m/s
Mass Flow rate (Q) Kg/s	39.87	79.748	119.65	159.5	199.38
Boutlet1 (Q1/Q)	0.071935	0.07307	0.07194	0.07151	0.07124
Boutlet2 (Q2/Q)	0.081608	0.08263	0.08161	0.07701	0.08103
Boutlet3 (Q3/Q)	0.090059	0.09094	0.09006	0.08975	0.08957
Boutlet4 (Q4/Q)	0.097858	0.09857	0.09786	0.09761	0.09747
Boutlet5 (Q5/Q)	0.104526	0.10501	0.10453	0.10436	0.10426
Boutlet6 (Q6/Q)	0.109795	0.10998	0.10979	0.10975	0.10975
Boutlet7 (Q7/Q)	0.113123	0.11300	0.11312	0.11321	0.11329
Boutlet8 (Q8/Q)	0.114662	0.11432	0.11466	0.11483	0.11497
Boutlet9 (Q9/Q)	0.111356	0.10930	0.11136	0.11198	0.11243
Boutlet10 (Q10/Q)	0.105221	0.10344	0.10522	0.10566	0.10610
Non-Uniformity Coefficient ϕ design 2	0.01307	0.01373	0.01374	0.01461	0.01417

Table 15: Non-Uniformity Coefficient Design 2

4.5 Effect of outlet on Flow Distribution

There have been ten simulations carried out using CFX Package to analyse the flow behaviour inside each design. The first simulation was the flow velocity at the entrance which was set to 1 m/s and increased by 1 after each set as follows 1 m/s, 2m/s….5 m/s. The main reason behind the increase in the inlet flow rate was to compare all the results and observe any change in the flow behaviour and distribution. However, according to the provided results and figures there wasn't any noticeable difference between all sets and each simulation showed nearly the same concept. Mass flow distribution figure 16 to figure 20 illustrates the same concept, the first four outlets have the lowest flow rate with 0.8%, 0.66%, 0.62% and 0.9% respectively. The flow distribution then starts increasing dramatically from 2% at outlet 5 to 29% at outlet 10.

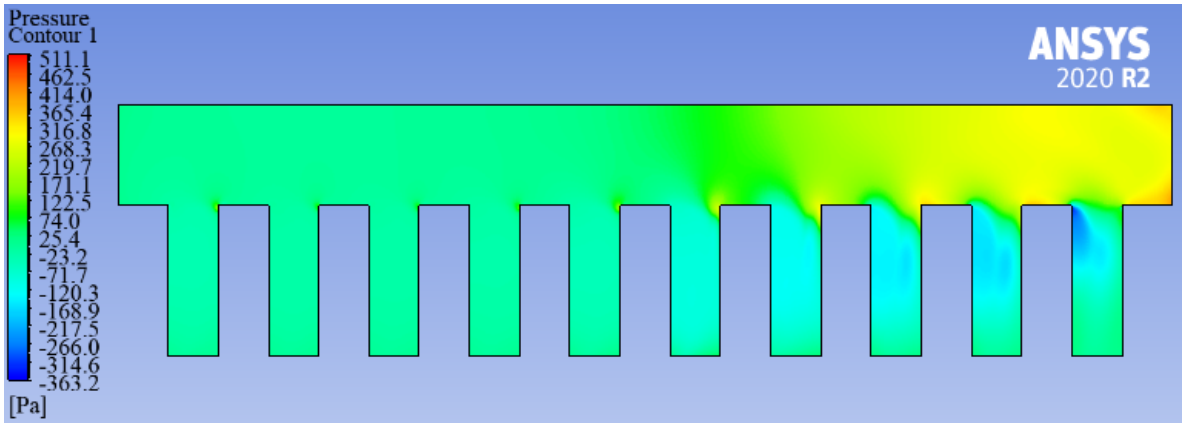

Figure 26: Low Pressure Distribution Design 1

The outlet flow ratio (Bout1, Bout2, Bout3 ….) is a measure of the flow distribution and shows how much fluid each outlet receives. Figures 22 and 23 represent the relation between outlet location and flow distribution for both design 1 and 2. As illustrated in Fig 22, all inlet flow rates for design 1 have shown similar pattern where outlet flow ratio is low at the first four outlets and increases sharply by the fifth, sixth, seventh until the end of the duct. As the flow enters the duct with high turbulent flow it leads to a flow type known as solo jet. This high momentum at the upper stream of the duct results in decreasing the static pressure thus lower pressure drop. However, once the axial momentum starts progressively decreasing the static pressure rises from the inlet towards the dead-end of the duct. This

rise in the static pressure leads to a higher efflux through the down-stream outlets. This interprets the similar distribution pattern for all inlet flow rate values.

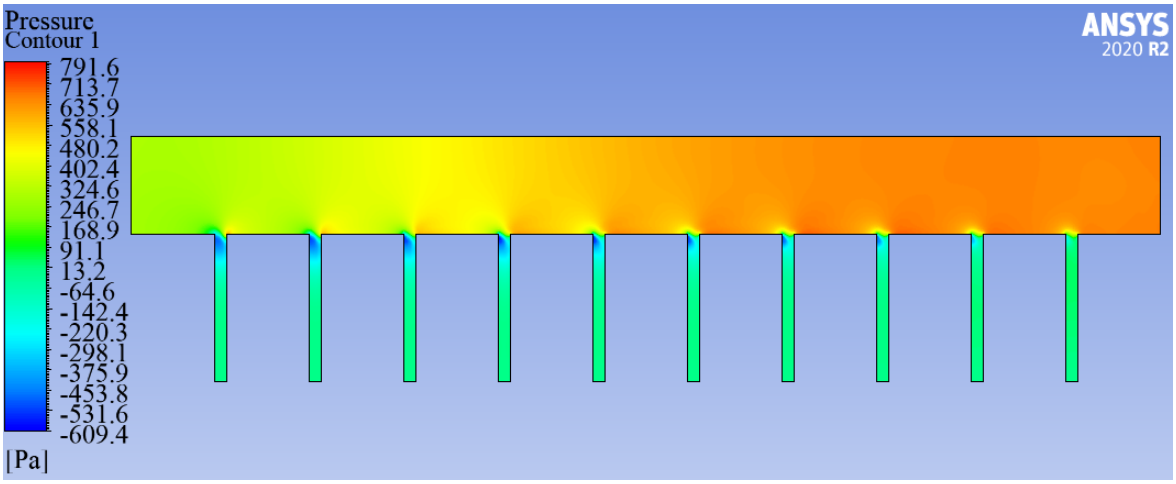

Figure 27: Increase in Pressure Distribution Contour Design 2

Figures 27 and 29 present a clear view of the pressure distribution inside the duct for Design 1 and Design 2. The static pressure is the direct influencer on the flow distribution. Momentum and friction are the main two factors that affect the pressure all over the duct. The friction impact occurs by reducing the pressure along the pipe whereas momentum raises the pressure. For Design 1, the fluid loss into outlets lead to a decrease in flow velocity that creates momentum deficiency over the dividing duct, consequently pressure rises over the end of the duct because of the conversion between energy (kinetic) and stagnation pressure.

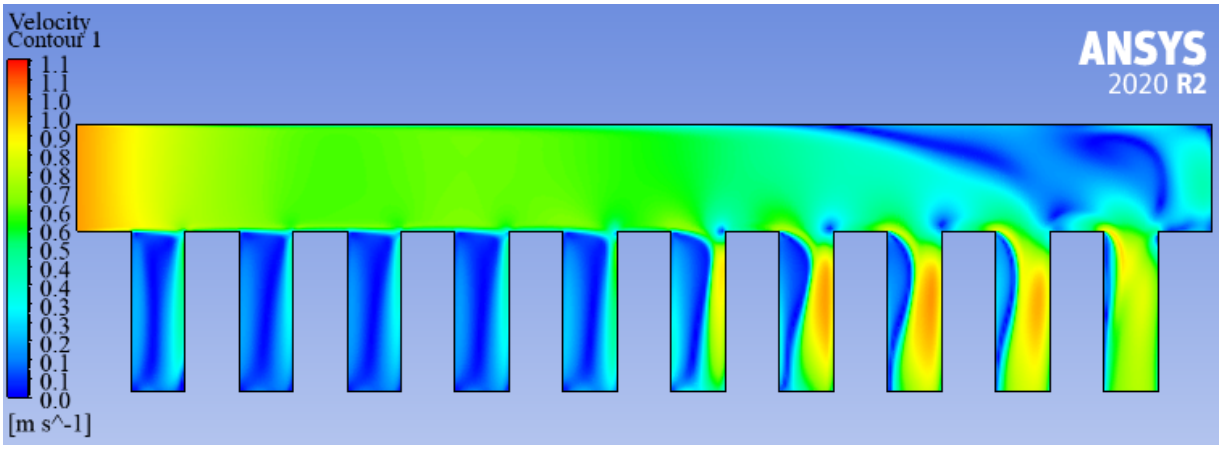

Figure 28: Design 1Velocity Distribution

Modifying the outlet size “Design 2” was an idea to observe its impact on flow distribution and non-uniformity. Figure 27 illustrates pressure contour for Design 2 where the pressure appears to be more uniform.

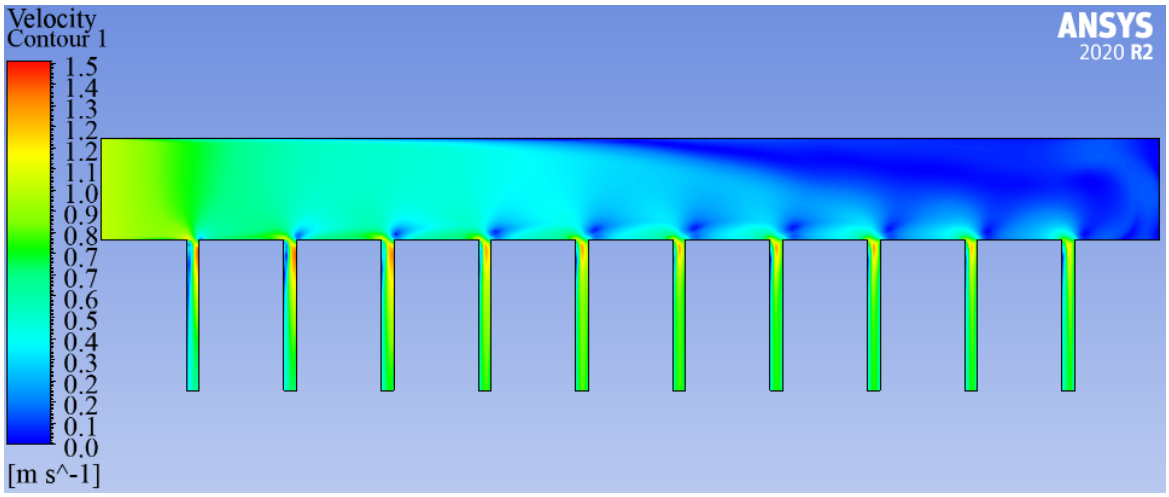

Figure 29: Outlet Reduction Effect on Flow Velocity

For Design 1 the highest-pressure value was 511 Pa and found at the duct dead end as shown in figure 26. Where the pressure for Design 2 has reached 791 Pa and was found at the duct centre due to the outlet reduction. It is also important to mention that the pressure at inlet in Design 1 starts with less than 10 Pa where in Design 2 it was probed and found 270 Pa at inlet. This remarkable increase in pressure at inlet for Design 2 explains the higher flow distribution and lower non-uniformity number provided by table 14 and 15. The lowest point of flow velocity for Design 1 was 0.02 m/s and probed at the first 5 outlets, the flow enters the duct with 1 m/s speed and continues with the same velocity to reach the last 5 outlets with 1 m/s flow speed. Figures 28 and 29 provide a clear description of the outlet size reduction effect towards the flow velocity. It is noticeable that outlet modification has resulted in significant impact on pressure and velocity distribution. The difference is obvious between the two designs as figures show and explains how design modification can results in considerable change. This rise in pressure must be carefully taken into consideration as some designs requires specific pressure limits. Thus, reaching the optimum design is a result of both reaching the most uniform flow as well as obtaining the design requirements and limitation.

4.6 Area ratio effect

Ratio of area is considered as the main factor in evaluating flow fluid uniformity through manifolds. It helps the designer to obtain the optimum design configuration by providing an appropriate measure as well as the most suitable fluid flow patterns. The area ratio for design 1 is 4.42 and 0.484 for Design 2, the relationship between non-uniformity coefficients and area ratio that figures show is obviously positive. The figures indicate that reducing area ratio has led to dramatic decrease in flow non-uniformity values for all various inlet flow rates. Increasing area ratio forces the flow to spread non-uniformly because of the decrease in static pressure as demonstrated in fig 22 and 23. The static pressure diminishes as a result of dynamic pressure rise which is responsible for fluid discharging through outlets. It is also important to mention that a higher number of outlets cause a loss in fluid energy due to many outlets edges which lead to sudden fluid expansion and contraction. Due to the

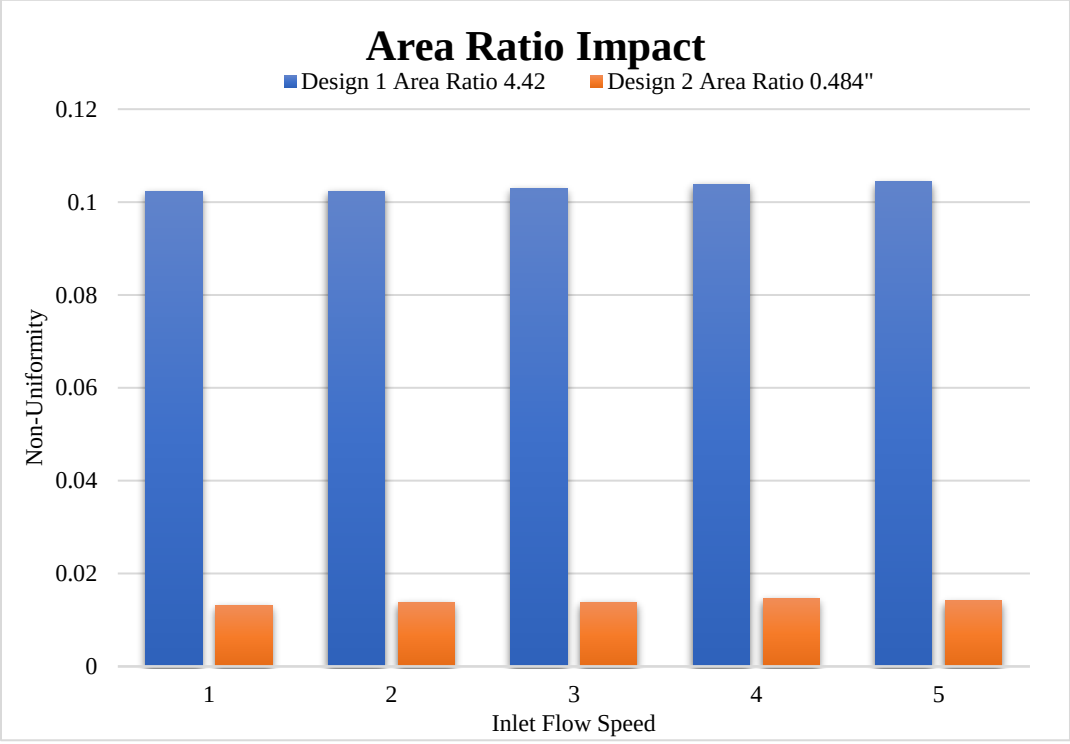

Figure 30: Area Ratio Effect on Non-Uniformity

number of different forces that can be acting on fluid particles and govern the flow pattern this explanation may not be sufficient to describe the relation between non-uniformity and area ratio. At 1m/s inlet flow rate, non-uniformity Φ was determined 10.23% for Design 1 area ratio and decreased

to reach 1.37% for Design 2 area ratio. The sharp decline in non-uniformity Φ from area ratio 1 to area ratio 2 is stupendous and it clearly indicates how non-uniformity is directly affected by area ratio. The provided observation is important and considered to be an appropriate feature to judge that an increment in area ratio would lead to an increase in non-uniformity Φ and hence at a specific value of area ratio the lowest flow distribution may be defined.

4.7 Inlet Flow rate effect on non-uniformity

Figures demonstrate the inlet flow rate effect on non-uniformity coefficient for both provided models. It is obvious to state that the graphs indicate positive relationship between higher inlet flow rate and increasing non-uniformity which Reynold number values also clarify. Increasing inlet flow rate leads to a rise in non-uniformity values, as a result of the small time period needed to allow the fluid to be distributed uniformly through the outlets. This occurs due to the significant fluid momentum by the Reynolds higher turbulence. Thus, fluid particles are pushed far from the first few outlets causing higher non-uniformity Φ.

Design 1					
Inlet Flow velocity	1 m/s	2 m/s	3 m/s	4 m/s	5 m/s
Reynolds number	224269.66	448539.3	672809	897078.6	1121348
Non-Uniformity (Φ) %	10.22%	10.23%	10.29%	10.38%	10.43%

Table 16: Inlet Flow Rate Effect on Non-Uniformity Design 1

Design 2					
Inlet Flow velocity	1 m/s	2 m/s	3 m/s	4 m/s	5 m/s
Reynolds number	224269.66	448539.3	672809	897078.6	1121348
Non-Uniformity (ϕ)%	1.307%	1.37%	1.37%	1.45%	1.42%

Table 17: Inlet Flow Rate Effect on Non-Uniformity Design 2

Figures 31 and 32 indicate inlet flow speed impact on non-uniformity (ϕ). For Design 1, non-uniformity continues to increase as inlet flow speed increases. This occurs due to the rise in turbulence once the flow enters the duct and as velocity rise pressure decreases and thus less flow distribution at the upstream.

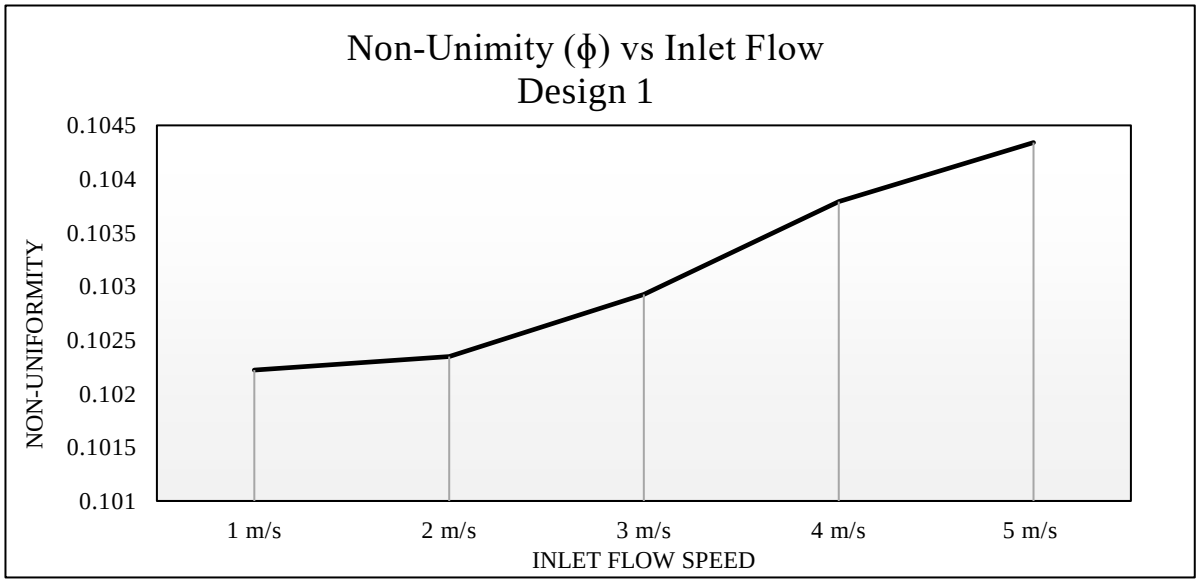

Figure 31: Inlet Flow Speed Impact on Non-uniformity Design 1

For Design 2 the situation is different, the increase in non-uniformity is mostly negligible "0.0005" this is because of the smaller area ratio impact. When the flow enters the duct with high flow speed the flow then faces modified "smaller" outlets at the downstream resulting in high pressure, forcing the flow to distribute equally at the upstream leading to higher uniformity all over the duct

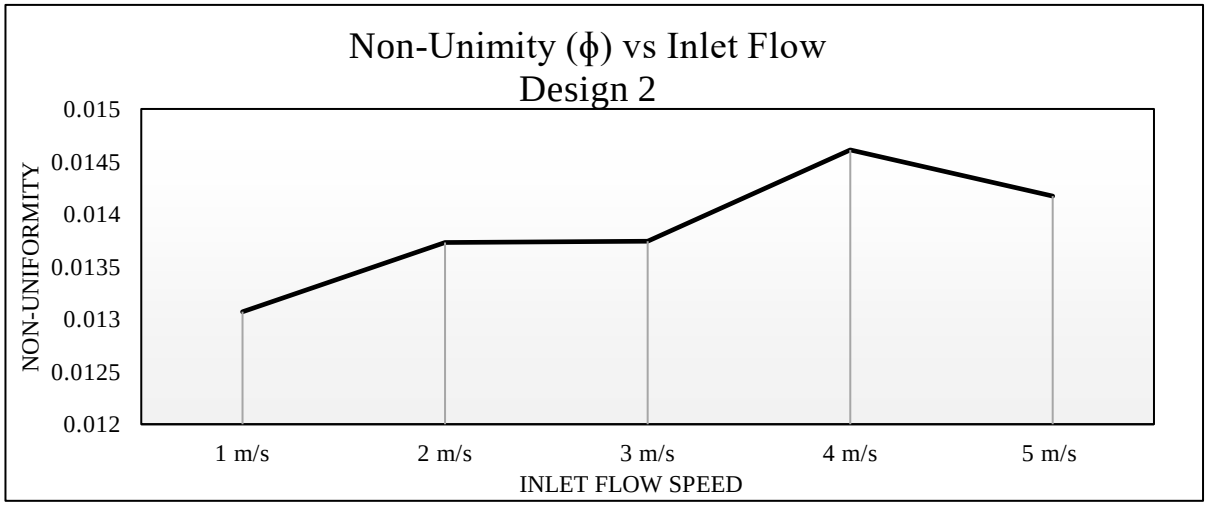

Figure 32: Inlet Flow Speed Impact on Non-uniformity Design 2

4.8 Results comparison

There are several research studies conducted in the past to improve flow distribution which mentioned in the literature. However, in this section only similar and promising studies will be discussed. 'The counter distributer offers a more uniform flow distribution than the parallel flow distributor applying the same geometric and operational conditions' (Datta and Majumdar, 1980). This statement supports the produced results that the geometrical effect plays a significant role towards the flow distribution, where different designs can optimise flow uniformity. However, it does not specify which geometrical part that mainly affect the distribution. Choi (1993) successfully identified the most important factor that agrees with the current study and results as he stated that area ratio (AR) is the most important parameter. However, Kim (1995) believes that the inlet shape and the flow rate are the two main factors that affect. Results presented in table 6-10 tend to agree with Choi over Kim as increasing or decreasing flow rate did not affect flow distribution. Hendrickson (2007) has developed a two-stage distribution structure to improve flow distribution in a heat exchanger and results have shown that the flow is more uniform when outlets size is equal to inlet. The obtained results would claim a similar view, however the relationship between inlet and outlet is complicated where large area ratio would indicate high non-uniformity. Thus, inlet and outlet size must not be equal if uniform flow is required. Anderson (2009) has numerically investigated the effect of outlet width and Reynolds number for liquid cooling configuration, and it was found that higher Reynold number lead to more flow in the last outlets and less flow in the first outlet. Table 17 stand against Anderson's study as Design 2 has shown better flow distribution even with high Reynold number. However, the results stand with the outlet width effect on flow distribution where figures indicate that outlet size is the main parameter in improving flow distribution. Outlet spacing and outlet size effect was performed using CFD by Hua (1998). He indicated that the flow tended to be more uniform with smaller width and larger length. Width of both Inlet and Outlet are the main two parameters and optimising such factors can contribute towards the overall flow distribution. Zhang and Li (2003) used gate-valve to tailor flow resistance achieving equal pressure drop at all outlets thus uniform flow inside the system. Such an

idea that only work for specific geometries and system and does not provide general solution. As literature shown, most researchers and studies tend to create special geometrical parameters to solve their own flow distribution issue, which stands against the work presented in this study. The idea is to provide a general solution that can successfully improve flow distribution.

CHAPTER FIVE

Conclusion

Generally, all the previous research with different applications have indicated that common manifold design does not lead to a uniform flow distribution at the outlets. Non-uniformity will be there where outlets closer to inlet will have less mass flow rate and farthest outlets from inlet will have the highest mass flow rate overall. End to end pressure is also affected accordingly and non-uniform pressure is produced. The reason as stated by numerous authors, is that the flow distribution is progressively consumed as a mass and is pulled out at every outlet. For uniform longitudinal distribution manifold, the axial momentum would progressively diminish. The static pressure increases as a result of this drop in momentum. An increase in the static pressure favours downstream outlets providing them with the highest flow rate along the manifold. In this thesis comprehensive research of previous studies was demonstrated for numerous flow distribution systems. There have been many approaches conducted to obtain equal flow rate through all outlets and to achieve uniformity. This thesis has tackled flow non-uniformity issues using a 3D numerical model known as Ansys Workbench. Parameters such as size of the outlets, flow velocity and area ratio have been investigated to observe their influence and increase uniformity and thus improve flow distribution. There are ten simulations of 3D numerical, turbulent, and incompressible fluid flow to distribute water fluid through 10 outlets. The results illustrate that area ratio has a direct effect on flow non-uniformity where Design 1 area ratio “4.42” has shown low flow distribution where the fluid discharged by 0.8% at the first outlet and 29% at the last outlet. This significant difference has dropped with Design 2 area ratio “0.484” where first outlet received 7% and 11% at the last outlet. Design 2 has clearly improved flow distribution where outlet size reduction has led to less flow non-uniformity. However, inlet flow velocity has shown a lower impact on flow distribution as increasing flow velocity didn’t have any noticeable change on results and its effect was negligible compared to area ratio. On the other hand, lower area ratio produces higher pressure inside the manifold which forces the fluid to exit the outlets

with high velocity and some designs have pressure and velocity thus, the two factors must be carefully taken into consideration.

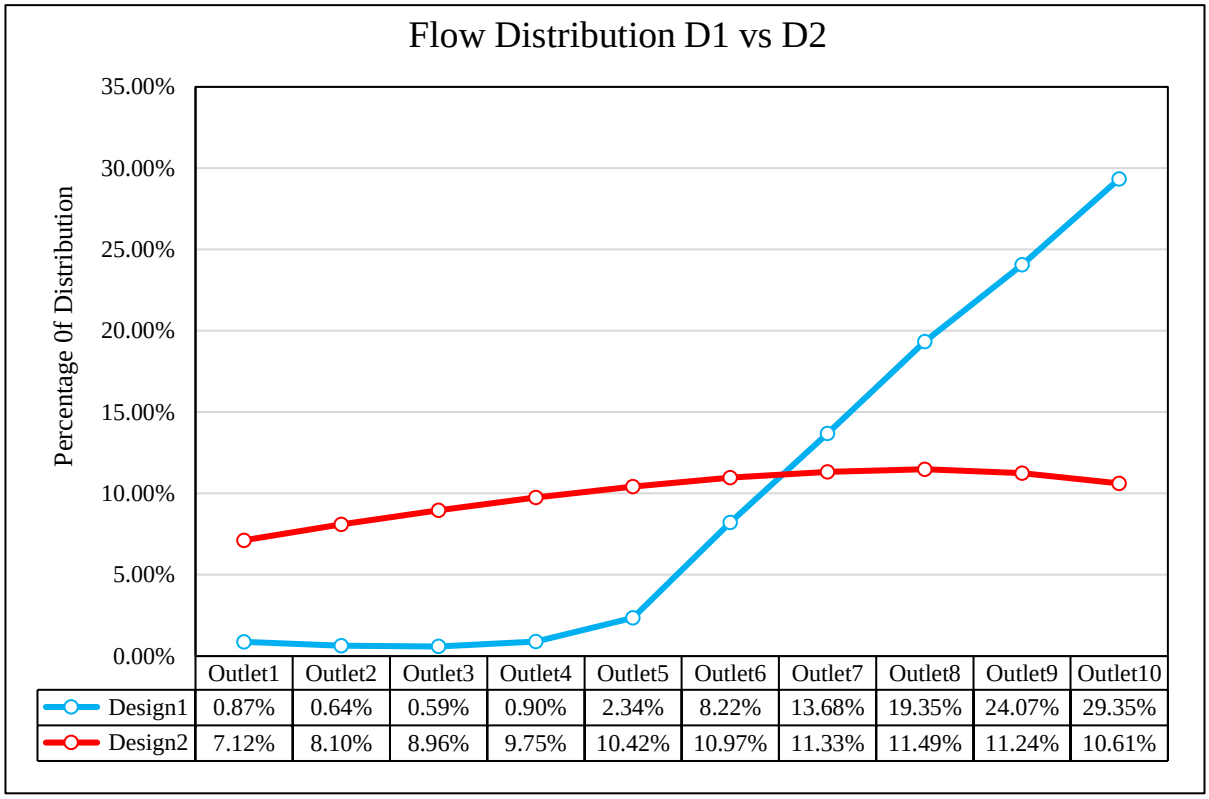

	Outlet1	Outlet2	Outlet3	Outlet4	Outlet5	Outlet6	Outlet7	Outlet8	Outlet9	Outlet10
Design1	0.87%	0.64%	0.59%	0.90%	2.34%	8.22%	13.68%	19.35%	24.07%	29.35%
Design2	7.12%	8.10%	8.96%	9.75%	10.42%	10.97%	11.33%	11.49%	11.24%	10.61%

Figure 33: Design 1 Flow Distribution vs Design 2 Flow Distribution

5.1 Future work

The conducted numerical simulations have demonstrated some serious results. However, experimental work is needed to support or stand against obtained results and figures. The numerical effect that outlet size reduction has shown towards flow distribution would lead to optimum manifold design if experimental work resulted present similar results and concepts produced numerically.

REFERENCES

Anderson, J. D., & Wendt, J. (2009). Computational Fluid Dynamics. New York: McGraw-Hil.

Andrew W. Chen, E. M. S. (2009). "Effect of Exitport Geometry on the Performance of a Flow Distribution Manifold." *Applied Thermal Engineering*.

Al Makky, A. (2021). Computational Fluid Dynamics is the Future. Retrieved 29 September 2021, from https://cfd2012.com/navier-stokes-equations.html

Aman, R. a. D., Yogesh and Raghuwanshi, Jitendra (2018). " Review on applications of computational fluid dynamics."

Batina, J., 2015. A gridless Euler/Navier-Stokes's solution algorithm for complex-aircraft applications. London, Sage, p. 333.

Bakker, A. a. H., Ahmad and Oshinowo, Lanre (2001). "Realize greater benefits from CFD." *Chemical Engineering Progress*.

Bajura, R. A., et al. (1974). "Fluid Distribution in Combining Dividing, and Reverse Flow Manifolds." Mechanical Engineering 96(2): 66-66.

Bajura, R. A., & Jones, E. H. (1978). Flow Distribution Manifolds. Journal of Fluids Engineering-Transactions of the Asme, 98(4), 654-666. doi:Doi 10.1115/1.3448441

Choi, S. H., Shin, S. Y., & Cho, Y. I. (1993a). The Effect of Area Ratio on the Flow Distribution in Liquid Cooling Module Manifolds for Electronic Packaging. International Communications in Heat and Mass Transfer, 20(2), 221-234. doi:Doi 10.1016/0735-1933(93)90050-6

Choi, S. H., Shin, S. Y., & Cho, Y. I. (1993b). The Effects of the Reynolds-Number and Width Ratio on the Flow Distribution in Manifolds of Liquid Cooling Modules for Electronic Packaging. International Communications in Heat and Mass Transfer, 20(5), 607-617. doi:Doi 10.1016/0735-1933(93)90073-5

Commenge, J. M., Falk, L., Corriou, J. P., & Matlosz, M. (2002). Optimal design for flow uniformity in microchannel reactors. Aiche Journal, 48(2), 345-358. doi:DOI 10.1002/aic.690480218

Datta, A.B., Majumdar, A.K. “Flow distribution in parallel and reverse flow manifolds” Int. J. Heat Fluid Flow 2 (1980) 253–262.

Durbin, P. A., & Reif, B. A. (2010). Reynolds Averaged Navier–Stokes Equations. . Statistical Theory and Modeling for Turbulent Flows, 45-56.

Griffini, G. M., & Gavriilidis, A. (2007). Effect of microchannel plate design on fluid flow uniformity at low flow rates. Chemical Engineering & Technology, 30(3), 395-406. doi:10.1002/ceat.200600324

Giraldo, G. (2020). "CFD Modeling, Analysis.". Retrieved 10/05/2020, 2020, from https://www.simscale.com/.

Guojiang, Wu & Song, Tan. (2005). CFD simulation of the effect of upstream flow distribution on the light-off performance of a catalytic converter. Energy Conversion and Management. 46. 2010-2031. 10.1016/j.enconman.2004.11.001.

Hendrickson, Grumman & Dino Roman, D. R., 2013. Drag: An Introduction. Applied Computational Aerodynamic, pp. 5-48.

Hoerner, S. F. (2012). Fluid-dynamic drag: practical information on aerodynamic drag and hydrodynamic resistance. London Hoerner Fluid Dynamics.

Hyper Physics. (2021). Reynolds Number. Retrieved from http://hyperphysics.phy-_astr.gsu.edhbase/pturb.html.

Hanfei Tuo a, Pega Hrnjak "Effect of the header pressure drop induced flow maldistribution on the microchannel evaporator performance", international journalof refrigeration 36 (2013) 2176-2186.

Hua, L. (1998). Computational Modeling of Manifold Type Flowspreaders. MSc Thesis, the University of Columbia,

Hudson, H. E., Uhler, R. B., & Bailey, R. W. (1979). Dividing-Flow Manifolds with Square-Edged Laterals. Journal of the Environmental Engineering Division-Asce, 105(4), 745-755. Retrieved from <Go to ISI>://WOS:A1979HL80500009

Jameson, A. (2008). Computational Fluid Dynamics and Airplane Design: Its current and Future impact. Retrieved from

Jimmy c. k. tong, development of systematic solution methodologies for the fluid-flow manifold problem, University of Minnesota, Ph.D. Dissertation, 2006

Jiao, A. J., Li, Y. Z., Chen, C. Z., & Zhang, R. (2003). Experimental investigation on fluid flow maldistribution in plate-fin heat exchangers. Heat Transfer Engineering, 24(4), 25-31. doi:10.1080/01457630390199715

Jones, G. F. a. J. M. G. (1998). "Isothermal flow distribution in coupled manifolds: Comparison of results from CFD and an integral model". Americtm Society of Mechanical Engineers, Fluids Engineering Division, Fairfield, NJ, 247

J.P. Chiou, The effect of nonuniform fluid flow distribution on the thermal performance of solar collector, Solar Energy 29 (1982).

Kim, S. Y., Choi, E., & Cho, Y. I. (1995). The Effect of Header Shapes on the Flow Distribution in a Manifold for Electronic Packaging Applications. International Communications in Heat and Mass Transfer, 22(3), 329-341. doi:Doi 10.1016/0735-1933(95)00024-S

Lu, F., Luo, Y. H., & Yang, S. M. (2008). Analytical and Experimental Investigation of Flow Distribution in Manifolds for Heat Exchangers. Journal of Hydrodynamics, 20(2), 179-185. doi:Doi 10.1016/S1001-6058(08)60044-X

McNown, J.S. "Mechanics of manifold flow" Transactions of ASCE, 119. pp. 1103-1142, 2008.

Maharudrayya, S., Jayanti, S., & Deshpande, A. P. (2005). Flow distribution and pressure drop in parallel-channel configurations of planar fuel cells. Journal of Power Sources, 144(1), 94-106. doi:10.1016/j.jpowsour.2004.12.018

Majumdar, A. K. (1980). Mathematical-Modeling of Flows in Dividing and Combining Flow Manifold. Applied Mathematical Modelling, 4(6), 424-432. doi:Doi 10.1016/0307-904x(80)90174-2

Mathew, B., John, T. J., & Hegab, H. (2009). Effect of Manifold Design on Flow Distribution in Multichanneled Microfluidic Devices. Fedsm2009, Vol 2, 543-548. Retrieved from <Go to ISI>://WOS:000282916200070

Mueller, A. C., Chiou, J.P. (1988). Review of various types of flow maldistribution in heat exchangers. Heat Trans. Engineering Education.

Pan, M., Zeng, D., Tang, Y., & Chen, D. (2009). CFD-based study of velocity distribution among multiple parallel microchannels. J. of Computers.

Pp.bme.hu.(2019). [online] Available at: https://pp.bme.hu/me/article/download/8518/6921/ [Accessed 16 Jul. 2019].

Pigford, R. L., Ashraf, M., & Miron, Y. D. (1983). Flow Distribution in Piping Manifolds. Industrial & Engineering Chemistry Fundamentals, 22(4), 463-471. doi:DOI 10.1021/i100012a019

Pretorius, W. A. (1997). Dividing-flow manifold calculations with a spreadsheet. Water Sa, 23(2), 147-150. Retrieved from <Go to ISI>://WOS:A1997WX66000006

Ramamurthy, A. S., Qu, J. Y., Vo, D., & Zhai, C. (2006). 3-d simulation of dividing flows in 90 deg rectangular closed conduits. Journal of Fluids Engineering-Transactions of the Asme, 128(5), 1126-1129. doi:10.1115/1.2243301

Rao, K. (2007). ANALYSIS OF FLOW MALDISTRIBUTION IN TUBULAR HEAT EXCHANGERS BY FLUENT. *National Institute Of Technology*.

Shen, P. I. (1992). The Effect of Friction on Flow Distribution in Dividing and Combining Flow Manifolds. Journal of Fluids Engineering-Transactions of the Asme, 114(1), 121-123. doi:Doi 10.1115/1.2909987

Solangi (2019). 02 conservation equations. [online] Slideshare.net. Available at: https://www.slideshare.net/aneessolangi/02-conservation-equations-68776953 [Accessed 10 Jun. 2019]

Temam, R., 2001. Navier-Stokes equations: theory and numerical analysis. American Mathematical Soc., p. 343.

Tu, J. (2018). Computational Fluid Dynamics. *ELSEVIER*. Retrieved from https://www.elsevier.com/books/computational-fluid-dynamics/tu/978-0-08-101127-0

Tong, J. C. K., Sparrow, E. M., & Abraham, J. P. (2009). Geometric strategies for attainment of identical outflows through all of the exit ports of a distribution manifold in a manifold system. Applied Thermal Engineering, 29(17-18), 3552-3560. doi:10.1016/j.applthermaleng.2009.06.010

Tonomura, O., Tanaka, S., Noda, M., Kano, M., Hasebe, S., & Hashimoto, L. (2004). CFD-based optimal design of manifold in plate-fin microdevices. Chemical Engineering Journal, 101(1-3), 397-402. doi:10.1016/j.cej.2003.10.022

Wen, J., Li, Y. Z., Zhou, A. M., & Ma, Y. S. (2006). PIV investigations of flow patterns in the entrance configuration of plate-fin heat exchanger. Chinese Journal of Chemical Engineering, 14(1), 15-23. doi:Doi 10.1016/S1004-9541(06)60032-3

Wikipedia, t. f. e. (2019). Flow distribution in manifolds. Retrieved from https://en.wikipedia.org/wiki/Flow_distribution_in_manifolds.

W. Slater, J. (2020). Uncertainty and Error in CFD Simulations. Retrieved 12 October 2022, from https://www.grc.nasa.gov/www/wind/valid/tutorial/errors.html.

Zhang, Z., & Li, Y. Z. (2003). CFD simulation on inlet configuration of plate-fin heat exchangers. Cryogenics, 43(12), 673-678. doi:10.1016/S0011-2275(03)00179-6

75(03)00179-6